Supporting Information for:

Reliably obtaining white light from layered halide perovskites at room temperature

Ethan J. Crace,[1] Alexander C. Su,[1] and Hemamala I. Karunadasa[1,2]*

1. Department of Chemistry, Stanford University, Stanford, California 94305, United States

2. Stanford Institute for Materials and Energy Sciences, SLAC National Accelerator Laboratory, Menlo Park, California 94025, United States.

* hemamala@stanford.edu

Abbreviations: BA = *n*-butylammonium, BzA = Benzylammonium, PEA = 2-phenethylammonium, MPenDA = 2-methyl-1,5-pentanediammonium, BDA = 1,4-butanediammonium, EDBE = 2,2'-(ethylenedioxy)bis(ethylammonium), API = 1-(3-ammoniopropyl)imidazolium, PZ = Piperazinium, IMA = 2-(ammoniomethyl)-1*H*-imidazol-3-ium, IEA = 2-(2-ammonioethyl)-1*H*-imidazol-3-ium, BIEA = 2-(2-ammonioethyl)-1*H*-benzimidazol-3-ium.

Experimental Methods

Unless otherwise noted, all manipulations were performed in air. All reagents were purchased at reagent grade or higher purity and used without further purification except for *o*-phenylenediamine, which was recrystallized from tert-butanol before use. Dimethyl sulfoxide (DMSO) was dried and degassed using a JC Meyer solvent purification system and was handled in a nitrogen-filled glovebox for spinning thin films.

Synthesis of BIEA·2Cl

Solid *β*-alanine (0.8 g, 9 mmol) and recrystallized *o*-phenylenediamine (1 g, 9 mmol) were placed in a 25 ml round bottom flask to which 6 ml of 6 M hydrochloric acid were added. A reflux condenser was attached and the solution was stirred and heated at reflux overnight. The colorless solution takes on a pink color, which darkens over time. The solution was allowed to cool to room temperature and was placed in a –20 °C freezer to induce precipitation of the product. The product was collected by filtration and was washed with acetone, which aided in removing colored impurities in the solid. If the material still had a colored impurity, the material was recrystallized out of 6 M HCl. Typically, the material, which appears pure by NMR, is colorless but the crude product is often pale pink in color. Yield: 60%. ^{1}H NMR (400 MHz, DMSO-d_6) δ 8.44 (s, 2H), 7.78 (m, 2H), 7.52 (m, 2H), 3.54 (t, J = 5.5 Hz, 2H), 3.50 (t, J = 5.8 Hz, 2H).

Synthesis of BIEA·2Br

The bromide salt of BIEA is prepared using the same method as for the chloride but 6 M hydrobromic acid is used as a solvent in the synthesis. It was also quite common for this synthesis to produce a dark blue color in solution and the crude material often has a pale blue color before purification. Yield: 60%. ^{1}H NMR (400 MHz, DMSO-d_6) δ 8.23 (s, 3H), 7.87 – 7.78 (m, 2H), 7.59 – 7.50 (m, 2H), 3.55 (t, J = 6.6 Hz, 2H), 3.46 (t, J = 6.7 Hz, 2H).

Preparation of Ammonium Chloride Salts

Chloride salts of BA, BzA, PEA, MPenDA, BDA, EDBE, and PZ were prepared by dissolving 0.4-0.6 mmol of the neutral amine in a minimal amount of dichloromethane. While the solution was stirred vigorously and cooled with an ice bath, a stoichiometric amount of 2 M HCl dissolved in diethyl ether was added drop wise. As the solution is added, a colorless solid precipitates. The solid was collected by filtration, dried under reduced pressure for 24 h, and stored in a desiccator under flowing dry air. Many of these salts are hygroscopic or deliquescent so storing in a dry atmosphere is essential.

Solid API·2Cl was prepared in a similar method, with the following small modification. After the addition of ethereal HCl, the ammonium salt precipitates but forms a sticky mass instead of a powder. The solvents were removed under reduced pressure and the resulting solid was dried overnight. The solid was then ground with a mortar and pestle and dried under reduced pressure again. The material was then stored in a desiccator under flowing nitrogen.

Synthesis of $(BzA)_2PbCl_4$

Crystals of this material were prepared by dissolving benzylamine (39.8 µL, 0.360 mmol) and $PbCl_2$ (50 mg, 0.18 mmol) in 2.1 ml of 6 M hydrochloric acid at 100 °C. Once the solids dissolved, the solution was cooled to room temperature at 3 °C/h. The resulting crystals were collected by filtration, washed with dibromomethane, and dried under reduced pressure overnight. The collected crystals were ground with a mortar and pestle before optical characterization.

Synthesis of $(PEA)_2PbCl_4$
Crystals of this material were prepared by dissolving phenethylamine (45.7 μL, 0.360 mmol) and $PbCl_2$ (50 mg, 0.18 mmol) in 2.1 ml of 6 M hydrochloric acid at 100 °C. Once the solids dissolved, the solution was cooled to room temperature at 3 °C/hr. The resulting crystals were collected by filtration, washed with dibromomethane, and dried under reduced pressure overnight. The collected crystals were ground with a mortar and pestle before optical characterization.

Synthesis of $(MPenDA)PbCl_4$
Crystals of this material were prepared by dissolving 2-methyl-1,5-pentanediamine (21.0 μL, 0.154 mmol) and $PbCl_2$ (43 mg, 0.15 mmol) in 12 M hydrochloric acid (1.5 ml) and allowing the solvent to slowly evaporate until colorless, plate-like crystals formed. These crystals were collected by filtration, washed thoroughly with dibromomethane, and then dried under reduced pressure overnight. The collected crystals were ground with a mortar and pestle before optical characterization.

Synthesis of $(BDA)PbCl_4$
Crystals of this material were prepared by dissolving 1,4-butanediamine (36 μL, 0.36 mmol) and $PbCl_2$ (100 mg, 0.360 mmol) in 12 M hydrochloric acid (4.5 ml) and allowing the solvent to slowly evaporate until colorless, plate-like crystals formed. These crystals were collected by filtration, washed thoroughly with dibromomethane, and then dried under reduced pressure overnight. The collected crystals were ground with a mortar and pestle before optical characterization.

Synthesis of $(EDBE)PbCl_4$
This material was prepared as a powder as previously reported[1] but precipitation was achieved by adding diethyl ether with vigorous stirring. This powder was collected by filtration, washed thoroughly with diethyl ether, and then dried under reduced pressure overnight.

Synthesis of $(PZ)PbCl_4$
This material was prepared as a powder by dissolving PZ·2Cl (114 mg, 0.721 mmol) and $PbCl_2$ (200 mg, 0.719 mmol) in enough 12 M HCl to dissolve the material and then adding diethyl ether with vigorous stirring. The powder was collected by filtration, washed with diethyl ether, and then dried under reduced pressure overnight.

Synthesis of $(API)PbCl_4$
Crystals of this material were prepared by dissolving API·2Cl (64 mg, 0.32 mmol) and $PbCl_2$ (88 mg, 0.32 mmol) in 3 ml of 12 M hydrochloric acid at room temperature and allowing diethyl ether to diffuse into the solution. The resulting crystals were collected by filtration, washed with dibromomethane, and dried under reduced pressure overnight. The collected crystals were ground with a mortar and pestle before optical characterization.

Synthesis of $(IMA)PbCl_4$
Crystals of this material were prepared by dissolving IMA·2Cl (18 mg, 0.10 mmol) and $PbCl_2$ (27 mg, 0.10 mmol) in 3 ml of 12 M hydrochloric acid. This solution was split into 1 ml portions and isopropyl alcohol was allowed to diffuse into the solutions over a few days to afford plate-like crystals. Occasionally, this solution also produces colorless needles of a different phase.

Phase pure powders of this material can be synthesized by dissolving 170 mg (1.00 mmol) of IMA·2Cl and 280 mg (1.01 mmol) of $PbCl_2$ in 10 ml of 12 M hydrochloric acid. With strong stirring, diethyl ether was then added to yield a colorless precipitate. The precipitate was filtered and washed liberally with additional diethyl ether. The sample was then dried under reduced pressure and stored in a desiccator. Anal. Calcd. for $(IMA)PbCl_4$: C: 10.27% H: 2.02% N: 9.38%. Found: C: 10.96% H: 2.22% N: 9.42%.

Synthesis of (IEA)$PbCl_4$
Crystals of this material were prepared by dissolving IEA·2Cl (27 mg, 0.15 mmol) and $PbCl_2$ (42 mg, 0.15 mmol) in 1.5 ml of 6 M hydrochloric acid at 100 °C. Once the solids dissolved, the solution was cooled to room temperature at 2 °C/hr. The resulting crystals were collected by filtration, washed with dibromomethane, and dried under reduced pressure overnight. The collected crystals were ground with a mortar and pestle before optical characterization. Anal. Calcd. for (IEA)$PbCl_4$: C: 13.00% H: 2.40% N: 9.09%. Found: C: 13.24% H: 2.22% N: 9.19%.

Synthesis of (BIEA)$PbCl_4$
Crystals of this material were prepared by dissolving BIEA·2Cl (35 mg, 0.15 mmol) and $PbCl_2$ (42 mg, 0.15 mmol) in 1.5 ml of 6 M hydrochloric acid at 100 °C. Once the solids dissolved, the solution was cooled to room temperature at 2 °C/hr. The resulting crystals were collected by filtration, washed with dibromomethane, and dried under reduced pressure overnight. The collected crystals were ground with a mortar and pestle before use. Anal. Calcd. for (BIEA)$PbCl_4$: C: 21.10% H: 2.56% N: 8.20%. Found: C: 21.36% H: 2.77% N: 8.42%.

Synthesis of (BIEA)$PbBr_4$
Crystals of this material were prepared by dissolving BIEA·2Br (33 mg, 0.10 mmol) and $PbBr_2$ (33 mg, 10 mmol) in 1.5 ml of 8.8 M hydrobromic acid at 100 °C. Once the solids dissolved, the solution was cooled to room temperature at 2 °C/hr. The resulting crystals were collected by filtration, washed with dibromomethane, and dried under reduced pressure overnight. The collected crystals were ground with a mortar and pestle before use. Anal. Calcd. for (BIEA)$PbBr_4$: C: 15.67% H: 1.90% N: 6.09%. Found: C: 15.55% H: 2.11% N: 6.25%.

Synthesis of $(PEA)_2PbCl_{4-x}Br_x$
The mixed-halide perovskites were prepared by mixing 55 mg (0.35 mmol) of PEA·Cl with 0.174 mmol of lead halide salts in 2 ml of a mixture of 6 M hydrochloric acid and 6 M hydrobromic acid (explicit ratios for the materials discussed in the manuscript are found below). The resulting mixture was heated to 100 °C to dissolve all solids. The solution was then cooled to room temperature at 1 °C/h. The resulting crystals were collected by filtration, washed with dibromomethane, and dried under reduced pressure overnight. The materials were ground to a fine powder using a mortar and pestle before optical characterization. All materials were stored in a desiccator when not in use.

The perovskite $(PEA)_2PbCl_{0.87}Br_{3.13}$ was prepared from a Cl:Br ratio of 1:1. Specifically, 55 mg (0.35 mmol) of PEA·Cl and 64 mg (0.17 mmol) $PbBr_2$ were dissolved in 1 ml of 6 M hydrochloric acid and 1 ml of 6 M hydrobromic acid.

The perovskite $(PEA)_2PbCl_{0.95}Br_{3.05}$ was prepared from a Cl:Br ratio of 3:2. Specifically, 55 mg (0.35 mmol) of PEA·Cl, 10 mg (0.035 mmol) of $PbCl_2$, and 51 mg (0.14 mmol) $PbBr_2$ were dissolved in 1.2 ml of 6 M hydrochloric acid and 0.8 ml of 6 M hydrobromic acid.

The perovskite $(PEA)_2PbCl_{1.44}Br_{2.56}$ was prepared from a Cl:Br ratio of 7:3. Specifically, 55 mg (0.35 mmol) of PEA·Cl, 19 mg (0.070 mmol) of $PbCl_2$, and 38 mg (0.10 mmol) $PbBr_2$ were dissolved in 1.4 ml of 6 M hydrochloric acid and 0.6 ml of 6 M hydrobromic acid.

The perovskite $(PEA)_2PbCl_{1.75}Br_{2.25}$ was prepared from a Cl:Br ratio of 4:1. Specifically, 55 mg (0.35 mmol) of PEA·Cl, 29 mg (0.10 mmol) of $PbCl_2$, and 26 mg (0.070 mmol) $PbBr_2$ were dissolved in 1.6 ml of 6 M hydrochloric acid and 0.4 ml of 6 M hydrobromic acid.

The perovskite $(PEA)_2PbCl_{2.81}Br_{1.19}$ was prepared from a Cl:Br ratio of 9:1. Specifically, 55 mg (0.35 mmol) of PEA·Cl, 39 mg (0.14 mmol) of $PbCl_2$, and 13 mg (0.035 mmol) $PbBr_2$ were dissolved in 1.8 ml of 6 M hydrochloric acid and 0.2 ml of 6 M hydrobromic acid.

Synthesis of (BDA)$PbCl_{4-x}Br_x$

Crystals of all perovskites were prepared by mixing 16 mg (0.099 mmol) of BDA·2Cl and 37 mg (0.10 mmol) of $PbBr_2$ in 1.5 ml of a mixture of 6 M hydrochloric and 6 M hydrobromic acid. The ratios of the acid solutions were 1:3, 1:1, and 3:1. All solutions were then heated to 100 °C and then allowed to cool to room temperature. Crystals were isolated by filtration, washed liberally with dibromomethane and diethyl ether, and dried under reduced pressure for several hours. The crystals were ground in a mortar and pestle before optical characterization.

Synthesis of (IEA)$PbCl_{4-x}Br_x$

Crystals of all perovskites were prepared by mixing 27 mg (0.15 mmol) of IEA·2Cl and 55 mg (0.15 mmol) of $PbBr_2$ in 1.5 ml of a mixture of 6 M hydrochloric and 6 M hydrobromic acid. The ratios of the acid solutions were 1:3, 1:1, and 3:1. All solutions were then heated to 100 °C and then allowed to cool to room temperature. Crystals were isolated by filtration, washed liberally with dibromomethane and diethyl ether, and dried under reduced pressure for several hours. The crystals were ground in a mortar and pestle before further use.

Synthesis of $(BA)_2PbCl_{0.73}Br_{3.27}$

Crystals of this material were prepared by combining 77 mg (0.70 mmol) of BA·Cl and 125 mg (0.341 mmol) of $PbBr_2$ in 1.5 ml of 6 M hydrochloric acid and 1.5 ml of 6 M hydrobromic acid. The mixed was heated to 100 °C until all solids dissolved. The solution was then cooled at 1 °C/h until the solution reached room temperature. The crystals were isolated by filtration, washed with dibromomethane, and dried under reduced pressure overnight. The crystals were then wet-milled in a ball mill with toluene (8 cycles; 1 cycle = 30 minutes at 500 rpm followed by a 30-minute pause) before being isolated by evaporating the toluene. The powder was stored in a desiccator.

Synthesis of (BIEA)$PbCl_{4-x}Br_x$

Powders of the mixed-halide perovskites were prepared by mixing 0.9 mmol of the combined BIEA halides and 0.9 mmol of the lead halides in 15 ml of a mixture of 6 M hydrochloric and 6 M hydrobromic acid (explicit ratios for the materials discussed in the manuscript are found below). The resulting mixture was heated to 100 °C with vigorous stirring until all solids dissolved. The stirred solution was then allowed to cool to room temperature. The resulting precipitates were stirred overnight, isolated by filtration, washed with diethyl ether, and then dried under reduced pressure overnight. All powders were wet-milled in a ball mill with toluene (3 cycles; 1 cycle = 30 minutes at 500 rpm followed by a 30-minute pause) and then stored in a desiccator.

The perovskite (BIEA)$PbCl_{1.83}Br_{2.17}$ was prepared from a Cl:Br ratio of 1:1. Specifically, 106 mg (0.453 mmol) BIEA·2Cl, 145 mg (0.449 mmol) BIEA·2Br, 125 mg (0.449 mmol) $PbCl_2$, and 165 mg (0.450 mmol) $PbBr_2$ were dissolved in 7.5 ml of 6 M hydrochloric acid and 7.5 ml of 6 M hydrobromic acid.

The perovskite (BIEA)$PbCl_{2.25}Br_{1.75}$ was prepared from a Cl:Br ratio of 3:1. Specifically, 160 mg (0.683 mmol) of BIEA·2Cl, 74 mg (0.23 mmol) of BIEA·2Br, 189 mg (0.679 mmol) of $PbCl_2$, and 84 mg (0.23 mmol) of $PbBr_2$ were dissolved in 11.25 ml of 6 M hydrochloric acid and 3.75 ml of 6 M hydrobromic acid.

Synthesis of $(BA)_2PbCl_{4-x}Br_x$

The mixed-halide perovskites, $(BA)_2PbCl_4$, and $(BA)_2PbBr_4$ were prepared by addition of 394 µl (4.00 mmol) of butylamine and 2.00 mmol of lead halide salts to a 20 ml vial, followed by rapid addition of first 9 M hydrobromic acid, then 12 M hydrochloric acid (explicit ratios for the materials discussed in the

manuscript are found below). The mixtures were capped and heated with vigorous stirring to dissolve all solids. During heating, significant bubbling and yellowing of the solutions was observed, so heating times were kept to a minimum. Once all solids were dissolved, the hot plate was turned off and the solution was cooled to room temperature overnight. The resulting crystals were collected by filtration, washed with dibromomethane, and dried under reduced pressure overnight. The materials were ground to a fine powder using a mortar and pestle before optical characterization. All materials were stored in a desiccator when not in use.

The perovskite $(BA)_2PbCl_4$ was prepared from a modified synthesis based on a previous report.[2] Specifically, 439 mg (4.00 mmol) of BA·Cl and 759 mg (2.00 mmol) of $Pb(CH_3COO)_2 \cdot 3H_2O$ were added to approximately 18 ml of 12 M HCl and dissolved while heating at 50 °C. No solids were observed after turning off the hot plate and allowing the solution to cool to room temperature. The solution was heated overnight at 100 °C and evaporated to dryness, yielding a colorless powder.

The "1:1 Cl:Br" ratio $(BA)_2PbCl_{4-x}Br_x$ material was prepared from a HCl:HBr ratio of 1:1. Specifically, 394 µl (4.00 mmol) of butylamine, 278 mg (1.00 mmol) of $PbCl_2$, and 367 mg (1.00 mmol) of $PbBr_2$ were dissolved in 4 ml of 12 M hydrochloric acid and 4 ml of 9 M hydrobromic acid. The resulting mixture was heated to 100 °C, with a total heating time of 18 minutes.

The perovskite $(BA)_2PbCl_{0.78}Br_{3.22}$ was prepared from a HCl:HBr ratio of 3:1. Specifically, 394 µl (4.00 mmol) of butylamine, 417 mg (1.50 mmol) of $PbCl_2$, and 184 mg (0.500 mmol) of $PbBr_2$ were dissolved in 6 ml of 12 M hydrochloric acid and 2 ml of 9 M hydrobromic acid. The resulting mixture was heated to 100 °C, with a total heating time of 18 minutes.

The perovskite $(BA)_2PbCl_{1.56}Br_{2.44}$ was prepared from a HCl:HBr ratio of 5:1. Specifically, 394 µl (4.00 mmol) of butylamine, 464 mg (1.67 mmol) of $PbCl_2$, and 121 mg (0.330 mmol) of $PbBr_2$ were dissolved in 6.67 ml of 12 M hydrochloric acid and 1.33 ml of 9 M hydrobromic acid. The resulting mixture was heated to a maximum temperature of 95 °C, with a total heating time of 13 minutes.

The perovskite $(BA)_2PbCl_{2.80}Br_{1.20}$ was prepared from a HCl:HBr ratio of 10:1. Specifically, 394 µl (4.00 mmol) of butylamine, 506 mg (1.82 mmol) of $PbCl_2$, and 66 mg (0.18 mmol) of $PbBr_2$ were dissolved in 7.27 ml of 12 M hydrochloric acid and 0.73 ml of 9 M hydrobromic acid. The resulting mixture was heated to a maximum temperature of 95 °C, with a total heating time of 13 minutes.

The perovskite $(BA)_2PbBr_4$ was prepared from a similar method to above. Specifically, 394 µl (4.00 mmol) of butylamine and 734 mg (2.00 mmol) of $PbBr_2$ were dissolved in 8 ml of 9 M hydrobromic acid. The resulting mixture was heated to 100 °C, with a total heating time of 18 minutes.

Thin-Film Preparation

All thin films were prepared in a nitrogen-filled glovebox to exclude moisture. Fused silica substrates were cut, scrubbed with a detergent solution, then sequentially sonicated in detergent, DI water, acetone, and isopropanol. The films were then dried with compressed air and treated with UV light and ozone for 20 minutes before being transferred into the glovebox for spinning. Film precursor solutions were prepared by dissolving a stoichiometric ratio of precursors in dimethylsulfoxide (0.125 M solution based on lead) in a nitrogen-filled glovebox. The solutions were heated to 80 °C and 80 µl of solution was then deposited on a fused silica substrate (1 cm × 1 cm) which was also held at 80 °C. The film was spun at 3000 rpm for 30 s followed by spinning at 5000 rpm for 50 s. The films were then annealed at 80 °C for 2 minutes. This method must be modified for the preparation of $(PZ)PbCl_4$. To prepare the spinning solution, equal volumes of ethylene glycol and dimethylsulfoxide were added to a stoichiometric ratio of precursors to prepare a

0.0625 M solution (if it had all dissolved). The solution was heated to 100 °C to produce a saturated solution. Not all of the solid (PZ)$PbCl_4$ dissolves at 100 °C so the solution is held at that temperature and the solution is carefully pipetted away from the solid to prepare the thin films. The substrates were still heated to 80°C before spinning and the resulting films were annealed at 80°C. All films were stored in a desiccator outside the glovebox before optical characterization. Note that (API)$PbCl_4$ films cannot be produced using this method.

Crystal Structure Determination

Crystals were coated with Paratone-N® oil, mounted on a Kapton® loop, and transferred to the Bruker D8 Venture diffractometer equipped with a Photon II detector. Frames were collected using ω and φ scans and unit-cell parameters were refined against all data. The crystals did not show significant decay during data collection. Frames were integrated and corrected for Lorentz and polarization effects using SAINT 8.34a[3] and were corrected for absorption effects using SADABS V2016/2.[4] Space-group assignments were based upon systematic absences, *E*-statistics, agreement factors for equivalent reflections, and successful refinement of the structures. Structures were solved using the intrinsic phasing method implemented in APEX3 v2018.7-2.[3, 5] Solutions were refined against all data using the SHELXL[6] software package and OLEX2.[7-8] Thermal parameters for all non-hydrogen atoms were refined anisotropically and the entire IMA molecule was modelled as disordered over two positions (180° rotation of the molecule). Hydrogen atoms were inserted at idealized positions and refined using a riding model with an isotropic thermal parameter 1.2 times that of the attached carbon or nitrogen atom.

For (IEA)$PbCl_4$, the single crystals are very commonly twinned (by non-merohedry). The twin domains (one major and one minor) for this crystal were found using CELL_NOW Version 2008/4,[9] which showed two domains rotated 180° about the *c** axis. The two cells were refined, integrated against all the data, and then absorption correction was performed using TWINABS Version 2012/1.[10] The data were solved as stated above using an hkl4 file but refined against the hkl5 file with a BASF of 0.2188(8). The IEA molecules were not disordered and required no additional treatment.

Both (BIEA)$PbCl_4$ and (BIEA)$PbBr_4$ structures are incommensurately modulated. The main peaks were separated from the satellites using the reciprocal space tools in Apex3. The main peaks were used to determine the unit cell. After finding the unit cell, the *q*-vector for the modulation was found using the incommensurate tool in Apex3. The data were first analyzed to find the average structure by using the method described above for non-modulated crystals without twinning. Part of the BIEA molecule (the primary amine and the adjacent carbon) must be modeled as being three-fold disordered. Some of the halide anions are also disordered over two positions. These structures, predictably, have large thermal ellipsoids and large maximum and minimum electron density peaks, which we attribute to the improper treatment of the modulation. The average structures at room temperature are better than the low-temperature structures due to the excess atomic vibrations masking some of the effects of modulation. Alternatively, the data were scaled as incommensurate and imported into Jana2006.[11] This procedure was used to obtain the superspace group and unit cell. The full solution is not complete, but sufficient for our analyses (See Table S3).

Powder X-ray Diffraction

PXRD measurements were performed under ambient conditions on a Bruker D8 Advance diffractometer equipped with a Cu anode ($K\alpha_1$ = 1.54060 Å, $K\alpha_2$ = 1.54443 Å, $K\alpha_2/K\alpha_1$ = 0.50000), fixed divergence slits with a nickel filter, and a LYNXEYE detector. The instrument was operated in a Bragg-Brentano geometry with a step size of 0.01° or 0.02° (2θ). Samples were prepared by suspending powder in toluene and depositing it on a glass slide to dry. The samples were then placed in an acrylic back-loading sample holder, which produces broad background peaks at 22.6° and 34° that appear in samples with relatively weaker diffraction. Additionally, some of the powder samples show a degree of preferential orientation. For materials with some preferential orientation, simulated powders patterns with March-Dollase parameters (*r*) of less than 1 are used to approximate the degree of preferential orientation.

Optical Measurements

Room- and low-temperature static photoluminescence spectra were acquired using a Horiba Jobin-Yvon Nanolog fluorimeter equipped with a 450-W xenon lamp and R928S detector. Samples were cooled using liquid nitrogen with a Janis ST-100H cryostat, with samples placed directly on the cold finger covered with AT205 Matt Black Foil Advanced Gaffa® Tape. Powder samples were prepared by first grinding crystals with a mortar and pestle or ball-milling using a Fritsch Pulverisette 7 planetary ball mill, followed by suspension in toluene with a solution of poly(methyl methacrylate) (average Mw ≈ 120,000 by GPC) in toluene. This slurry was then allowed to dry at room temperature. Excitation wavelengths between 290-365 nm were used. We observed minimal differences in emission spectrum peak center and band shape with these excitation energies. Excitation wavelengths were chosen to optimize the emission signal-to-noise ration and to accommodate long pass filters used to filter out the excitation wavelength scattering from powder samples.

Room-temperature absorption measurements of thin-film samples were taken using an Agilent Cary 6000i spectrometer in transmission mode. All scans have a source change from a deuterium arc lamp to a quartz iodide lamp at 350 nm (3.54286 eV). This source change can cause a step-like artifact in the data, which was not removed.

Photoluminescence quantum efficiency (PLQE) measurements were acquired using the same Horiba Jobin-Yvon Nanolog fluorimeter as described above with a Horiba K-sphere integrating sphere attachment with a powder sample holder using stainless-steel screws to reduce fluorescent background. The integrating sphere walls are known to exhibit weak photoluminescence, which introduces a non-constant background that is convoluted with the sample PL during measurements.[12] For samples with low PLQE, such as the samples measured here, this causes a systematic error that can be a significant fraction of the calculated PLQE. The ratio of excitation peak intensities of the sample and reference blank were taken and applied to the reference blank emission spectrum as a correction to account for this error. Instrument and sphere corrections were applied and the PLQE was calculated with the formula $\eta = \frac{E_c - E_a}{L_a - L_c}$, where E_c and E_a are the integrated emission intensities of the sample and blank, respectively, and L_a and L_c are the integrated excitation intensities of the blank and sample, respectively.

ICP-MS and Elemental Analysis

Chemical analysis of Br and Pb content was obtained by inductively coupled plasma mass spectrometry (ICP-MS) using a Thermo XSeries II ICP-Mass Spectrometer operated by the Stanford Environmental Measurement Facility (EMF). Values for x in the formulas of (PEA)$PbCl_{4-x}Br_x$, (BIEA)$PbCl_{4-x}Br_x$, and $(BA)_2PbCl_{4-x}Br_x$ were determined by taking the ratio of the lead and bromide concentrations (obtained in triplicate for accuracy). For (PEA)$PbCl_{4-x}Br_x$ and (BIEA)$PbCl_{4-x}Br_x$, the mixed-halide compounds were dissolved in a matrix of 1.4% HNO_3 solution in DI water. For $(BA)_2PbCl_{4-x}Br_x$, the compounds were dissolved in a matrix of 2% HNO_3 solution in MilliQ water. Other perovskites with mixed halides are provided with the ratio of halides that were present in the perovskite growth solution. C, H, and N analysis was performed by MHW Laboratories (Phoenix, AZ) on ground solid samples.

Calculation of Intraoctahedral and Interoctahedral Parameters

The value of the out-of-plane interoctahedral distortion (D_{out}) for the seven (001) perovskites was calculated using a slight modification of the Matlab script "PbBrAngles_withouterror.m" previously published by Smith, Jaffe, Karunadasa et al.[13] The only modification to the script was the replacement of all instances of "Br" with "Cl" so that the script would properly read the .xyz files containing the atomic positions. Atoms were treated as vectors by using their Cartesian coordinates derived from single-crystal X-ray structures. In order to calculate D_{out}, planes were defined by three Pb atoms rather than crystallographic planes because in certain cases, the Pb atoms do not lie exactly in the (001) plane.

All intraoctahedral parameters were determined by examining each crystallographically unique lead site and measuring distances and angles within the octahedron around that lead atom. In cases where more than one crystallographically unique lead was present or when halides were disordered over multiple positions, every possible unique octahedron was measured and the smallest or largest value for each parameter was recorded for further analysis. Interoctahedral Pb–Pb distance was measured by examining the distance between each lead atom in a 2 × 2 × 2 supercell to find the shortest distance. The shortest interoctahedral Cl–Cl distance was determined by using this supercell approach as well, but all distances that were shorter than or equal to the longest intraoctahedral Cl–Cl distance were intraoctahedral interactions and were discarded before selecting the shortest interoctahedral Cl–Cl distance.

Octahedral distortion parameters were calculated based on Cartesian coordinates obtained from a crystallographically unique lead atom and the 6 halides that are octahedrally coordinated to the metal. Multiple parameters to determine octahedral distortion have been proposed. In this study we examined 4 measures of octahedral distortion: S, Δ_{oct}, σ^2_{oct}, and λ_{oct}. The S parameter was determined by the program *SHAPE*.[14] The program calculates continuous shape measures for the input atomic positions with reference to an idealized polyhedron based on minimal distortion paths,[15] generalized interconversion coordinates,[16] and the following algorithm:[17]

$$S = \min \frac{\sum_{k=1}^{N} |Q_k - P_k|^2}{\sum_{k=1}^{N} |Q_k - Q_0|^2} \times 100$$

where S is a dimensionless continuous symmetry measure obtained by assessing the root-mean-square (rms) deviation of the N vertices from their idealized positions. The vector Q_k contains the coordinates of the N vertices, P_k is the vector for the idealized positions, and Q_0 is the coordinate vector of the center of mass. S is normalized by the rms distance from the center of mass to all the vertices to avoid size effects.

The parameter Δ_{oct} measures the deviation of individual metal-halide bonds from the average bond distance as defined by the following equation:[18]

$$\Delta_{oct} = \frac{1}{6} \sum_{n=1}^{6} \left[\frac{(d_n - d_{avg})}{d_{avg}} \right]^2$$

where each value of n indexes one of the M–X bonds in the octahedron, d_n is the distance of an individual M–X bond, and d_{avg} is the average value of the bond distances of the M–X bonds in the octahedron. Note that this distortion parameter contains no information about deviation from ideal bond angles. Deviations of cis X–M–X bond angles in an octahedron can be determined by calculation of σ^2_{oct}. This distortion parameter calculates the variance of the cis X–M–X bond angles from the ideal value of 90° :[19]

$$\sigma^2_{oct} = \frac{1}{11} \sum_{n=1}^{12} (\theta_n - 90)^2$$

where each value of n indexes an individual cis X–M–X bond angle, and θ_n is the value of the angle in degrees. Note for this sum, Bessel's correction was applied to reduce error in population variance due to a finite sample (hence the prefactor of $1/(n-1) = 1/11$). Also note there is no bond length information in this calculation. The final octahedral distortion parameter, λ_{oct}, is similar to S but is a simplified calculation. The following summation is used to calculate λ_{oct}:[19]

$$\lambda_{\mathrm{oct}} = \frac{1}{6}\sum_{\mathrm{n}=1}^{6}\left(\frac{d_{\mathrm{n}}}{d_0}\right)^2$$

where d_{n} is define in the same manner as in Δ_{oct} and d_0 is the M–X bond length in an idealized octahedron with the same volume as the distorted octahedron being examined. The volume of the octahedron being examined must be calculated as the sum of the volumes of 8 irregular tetrahedra into which the octahedron can be divided. The vertices of each tetrahedron are defined by the central metal atom and three halides which share a face of the octahedron. Because the distance between the vertices of the tetrahedron (i.e., the interatomic distances) can be found from the crystallographic information, the volume of these irregular tetrahedra can be calculated using a Cayley-Menger determinant:[20]

$$288\,V_{\mathrm{tet}}^2 = \begin{vmatrix} 0 & 1 & 1 & 1 & 1 \\ 1 & 0 & d_{12}^2 & d_{13}^2 & d_{14}^2 \\ 1 & d_{12}^2 & 0 & d_{23}^2 & d_{24}^2 \\ 1 & d_{13}^2 & d_{23}^2 & 0 & d_{34}^2 \\ 1 & d_{14}^2 & d_{24}^2 & d_{34}^2 & 0 \end{vmatrix}$$

where V_{tet} is the volume of a single tetrahedron with vertices represented by the subscripts $i,j \in (1,2,3,4)$ and d_{ij} is the distance between the vertices. After solving for volume of the octahedron (the sum of all values of V_{tet} in the octahedron), the value for d_0 can be found by combining the formula for the volume of a regular octahedron and the Pythagorean theorem which relates the cis X–X distance and d_0:

$$d_0 = \frac{d_{\mathrm{XX}}}{\sqrt{2}} = \sqrt[3]{\frac{3V_{\mathrm{oct}}}{4}}$$

where V_{oct} is the volume of the irregular octahedron and d_{XX} is the cis halide-halide distance in the ideal octahedron.

Table S1. Crystallographic data for (001) perovskites $(IMA)PbCl_4$ and $(IEA)PbCl_4$

	$(IMA)PbCl_4$		$(IEA)PbCl_4$[a]	
Empirical Formula	$C_4N_3H_9PbCl_4$	$C_4N_3H_9PbCl_4$	$C_5N_3H_{11}PbCl_4$	$C_5N_3H_{11}PbCl_4$
Formula Weight, $g \cdot mol^{-1}$	448.13	448.13	462.16	462.16
Temperature, K	100	300	100	300
Crystal System	Orthorhombic	Orthorhombic	Monoclinic	Monoclinic
Space group	*Pbca*	*Pbca*	$P2_1/c$	$P2_1/c$
a, Å	15.7175(5)	15.7952(8)	9.6565(5)	9.7314(4)
b, Å	8.1812(2)	8.1952(4)	11.2444(5)	11.3143(4)
c, Å	17.2809(6)	17.4241(10)	11.4494(5)	11.5207(5)
α , °	90	90	90	90
β , °	90	90	106.444(2)	106.608(2)
γ , °	90	90	90	90
Volume, $Å^3$	2222.12(12)	2255.5(2)	1192.34(10)	1215.56(9)
Z	8	8	4	4
Density (calc), $g \cdot cm^{-3}$	2.679	2.639	2.575	2.525
Absorption coef., mm^{-1}	16.101	15.863	15.007	14.721
F(000)	1632.0	1632.0	848.0	848.0
Crystal size, mm^3	0.06 × 0.05 × 0.018	0.06 × 0.05 × 0.018	0.2 × 0.11 × 0.03	0.2 × 0.11 × 0.03
Radiation	Mo Kα	Mo Kα	Mo Kα	Mo Kα
2θ range, °	5.184 to 54.206	4.676 to 50.698	4.398 to 56.62	5.156 to 56.638
Index ranges	$-20 \le h \le 20$ $-10 \le k \le 10$ $-22 \le l \le 22$	$-19 \le h \le 19$ $-9 \le k \le 9$ $-20 \le l \le 20$	$-12 \le h \le 12$ $0 \le k \le 14$ $0 \le l \le 15$	$-12 \le h \le 12$ $0 \le k \le 15$ $0 \le l \le 15$
Reflections collected/ Independent reflections	43232/2456	50954/2061	5494/5494	4837/4837
R_{int}, R_{sigma}	0.0700, 0.0222	0.0750, 0.0192	NA, 0.0376	NA, 0.0300
Data/restraints/parameters	2456/141/144	2061/333/174	5494/0/120	4837/0/120
Goodness-of-fit on F^2	1.049	1.179	1.065	1.164
Final *R* indices $[I > 2\sigma(I)]$[a]	$R_1 = 0.0176$ $wR_2 = 0.0333$	$R_1 = 0.0204$ $wR_2 = 0.0474$	$R_1 = 0.0343$ $wR_2 = 0.0751$	$R_1 = 0.0380$ $wR_2 = 0.1186$
R indices (all data)[b]	$R_1 = 0.0338$ $wR_2 = 0.0390$	$R_1 = 0.0399$ $wR_2 = 0.0574$	$R_1 = 0.0447$ $wR_2 = 0.0828$	$R_1 = 0.0479$ $wR_2 = 0.1266$
Largest diff. peak and hole, $e \cdot Å^{-3}$	0.55, –1.13	0.50, –1.37	1.31, –2.30	1.99, –1.93

[a] $(IEA)PbCl_4$ very commonly twins and this particular crystal had two twin domains. See experimental section discussing crystallography.

[b] $R_1 = \Sigma||F_o| - |F_c||/\Sigma|F_o|$, $wR_2 = [\Sigma w(F_o^2 - F_c^2)^2/\Sigma(F_o^2)^2]^{1/2}$

Table S2. Crystallographic data for (110) perovskites (BIEA)$PbCl_4$ and (BIEA)$PbBr_4$

	(BIEA)$PbCl_4$[a]		(BIEA)$PbBr_4$[a]	
Empirical Formula	$C_9N_3H_{13}PbCl_4$	$C_9N_3H_{13}PbCl_4$	$C_9N_3H_{13}PbBr_4$	$C_9N_3H_{13}PbBr_4$
Formula Weight, g·mol^{-1}	512.21	512.21	690.05	690.05
Temperature, K	100	300	100	300
Crystal System	Monoclinic	Monoclinic	Monoclinic	Monoclinic
Space group	*C*2/*c*	*C*2/*c*	*C*2/*c*	*C*2/*c*
a, Å	11.4711(7)	11.5223(3)	11.9594(5)	12.0291(2)
b, Å	30.4656(19)	30.5566(9)	30.9963(17)	31.1120(7)
c, Å	8.3810(5)	8.4574(2)	8.6387(5)	8.7353(2)
α , °	90	90	90	90
β , °	93.624(2)	93.4720(10)	94.1860(10)	94.0590(10)
γ , °	90	90	90	90
Volume, Å^3	2923.1(3)	2972.24(14)	3193.8(3)	3260.98(12)
Z	8	8	8	8
Density (calc), g·cm^{-3}	2.328	2.289	2.870	2.811
Absorption coef., mm^{-1}	12.256	12.054	20.557	20.134
F(000)	1904.0	1904.0	2480.0	2480.0
Crystal size, mm^3	0.07 × 0.03 × 0.01	0.07 × 0.03 × 0.01	0.165 × 0.065 × 0.015	0.165 × 0.065 × 0.015
Radiation	Mo Kα	Mo Kα	Mo Kα	Mo Kα
2θ range, °	3.8 to 54.97	3.784 to 54.2	5.216 to 54.97	3.638 to 52.744
Index ranges	$-14 \le h \le 14$ $-39 \le k \le 39$ $-9 \le l \le 10$	$-14 \le h \le 14$ $-39 \le k \le 39$ $-10 \le l \le 10$	$-15 \le h \le 15$ $-40 \le k \le 40$ $-11 \le l \le 11$	$-15 \le h \le 14$ $-38 \le k \le 38$ $-10 \le l \le 10$
Reflections collected/ Independent reflections	38289/3349	41153/3284	42973/3677	38217/3331
R_{int}, R_{sigma}	0.0590, 0.0282	0.0460, 0.0177	0.0544, 0.0257	0.0588, 0.0270
Data/restraints/parameters	3349/266/192	3284/326/204	3677/218/190	3331/218/204
Goodness-of-fit on F^2	1.279	1.093	1.242	1.022
Final *R* indices [$I > 2\sigma(I)$][a]	$R_1 = 0.0575$ w$R_2 = 0.1202$	$R_1 = 0.0246$ w$R_2 = 0.0470$	$R_1 = 0.0637$ w$R_2 = 0.1442$	$R_1 = 0.0296$ w$R_2 = 0.0684$
R indices (all data)[b]	$R_1 = 0.0603$ w$R_2 = 0.1213$	$R_1 = 0.0292$ w$R_2 = 0.0484$	$R_1 = 0.0684$ w$R_2 = 0.1464$	$R_1 = 0.0380$ w$R_2 = 0.0730$
Largest diff. peak and hole, e·Å^{-3}	2.97, –6.64	1.01, –1.33	2.79, –4.24	1.46, –1.47

[a]Both of these materials are modulated structures. The crystal structure given here is the average structure for the materials. See experimental section discussing crystallography and Table S3.

[b]$R_1 = \Sigma||F_o| - |F_c||/\Sigma|F_o|$, w$R_2 = [\Sigma w(F_o^2 - F_c^2)^2/\Sigma(F_o^2)^2]^{1/2}$

Table S3. Modulation information for (110) perovskites (BIEA)$PbCl_4$ and (BIEA)$PbBr_4$

	(BIEA)$PbCl_4$		(BIEA)$PbBr_4$	
Empirical Formula	$C_9N_3H_{13}PbCl_4$	$C_9N_3H_{13}PbCl_4$	$C_9N_3H_{13}PbBr_4$	$C_9N_3H_{13}PbBr_4$
Temperature, K	100	300	100	300
Dimensions	3+1	3+1	3+1	3+1
Superspace group	$C2/c(\alpha,0,\gamma)0s$	$C2/c(\alpha,0,\gamma)0s$	$C2/c(\alpha,0,\gamma)0s$	$C2/c(\alpha,0,\gamma)0s$
q-vector	(–0.21403, 0, 0.38440)	(–0.21403, 0, 0.38440)	(–0.24674, 0, 0.36141)	(–0.27416, 0, 0.36100)
Satellite Order	1 (weak)	1 (weak)	2 (2^{nd} very weak)	1

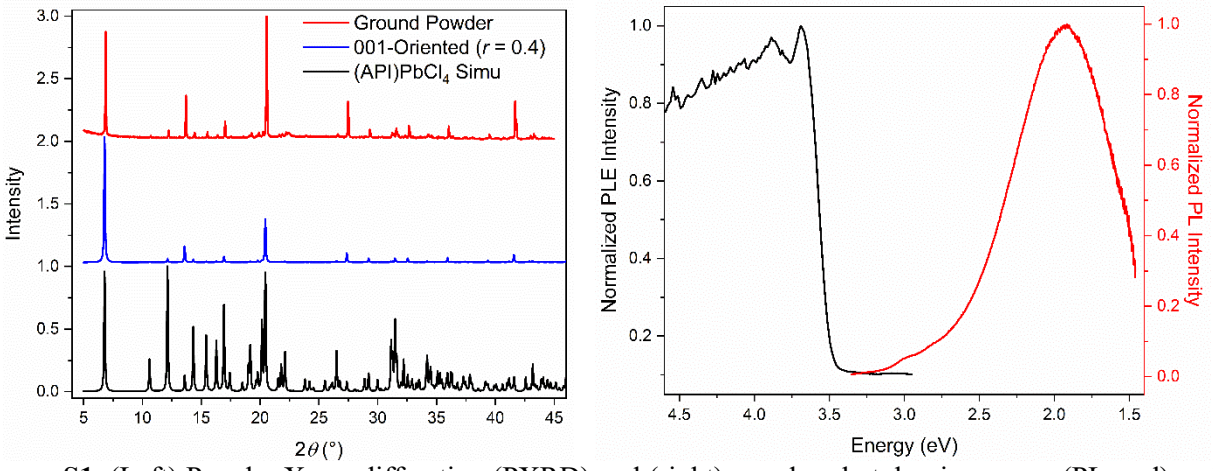

Figure S1. (Left) Powder X-ray diffraction (PXRD) and (right) powder photoluminescence (PL; red) and photoluminescence excitation (PLE; black) of (API)$PbCl_4$

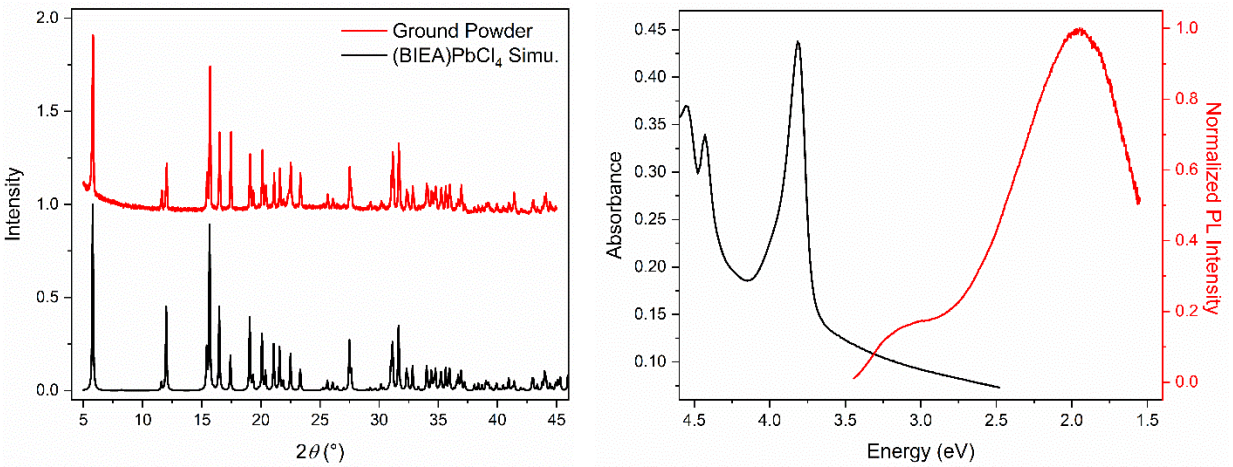

Figure S2. (Left) PXRD and (right) thin-film absorption (black) and powder PL (red) of (BIEA)$PbCl_4$

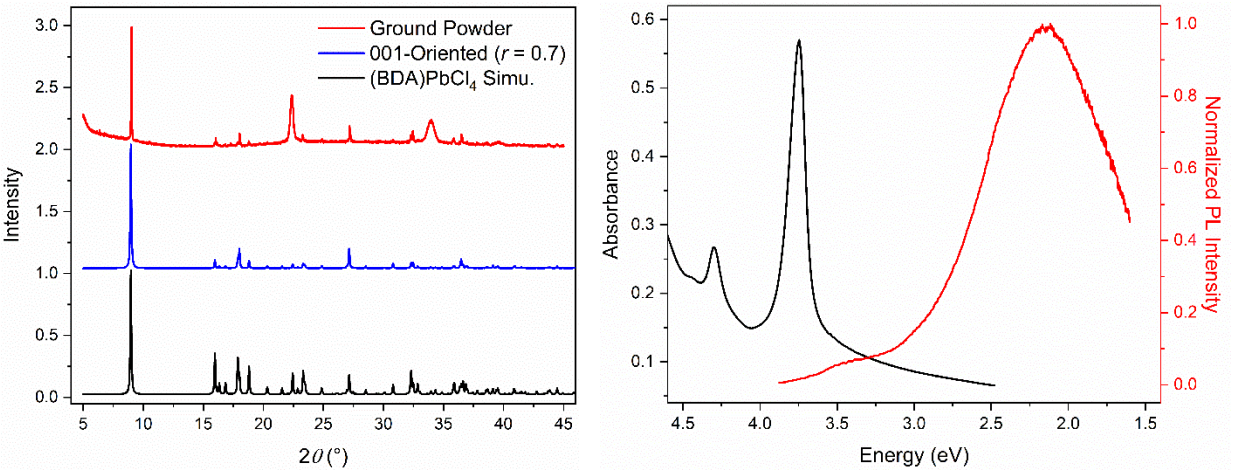

Figure S3. (Left) PXRD and (right) thin-film absorption (black) and powder PL (red) of (BDA)$PbCl_4$

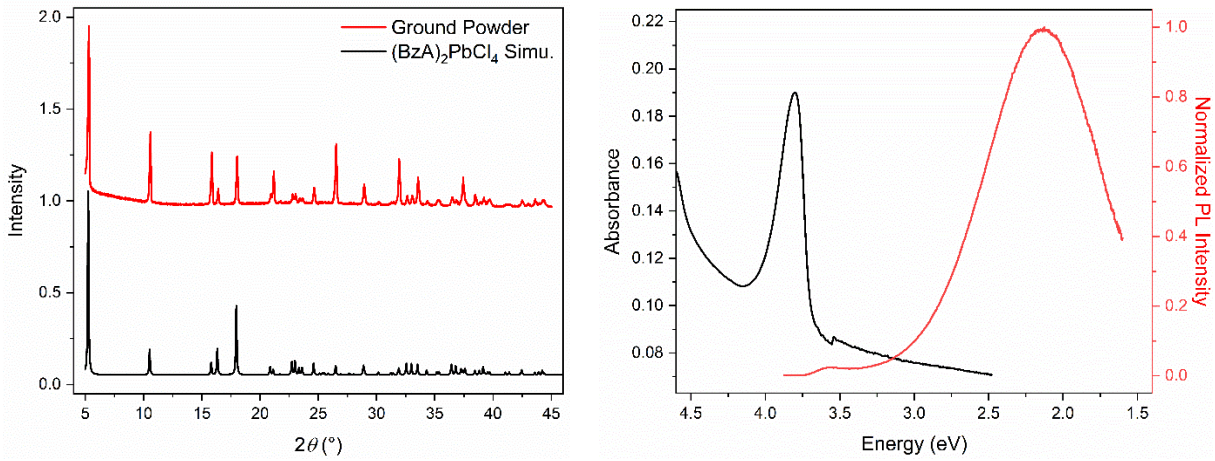

Figure S4. (Left) PXRD and (right) thin-film absorption (black) and powder PL (red) of $(BzA)_2PbCl_4$

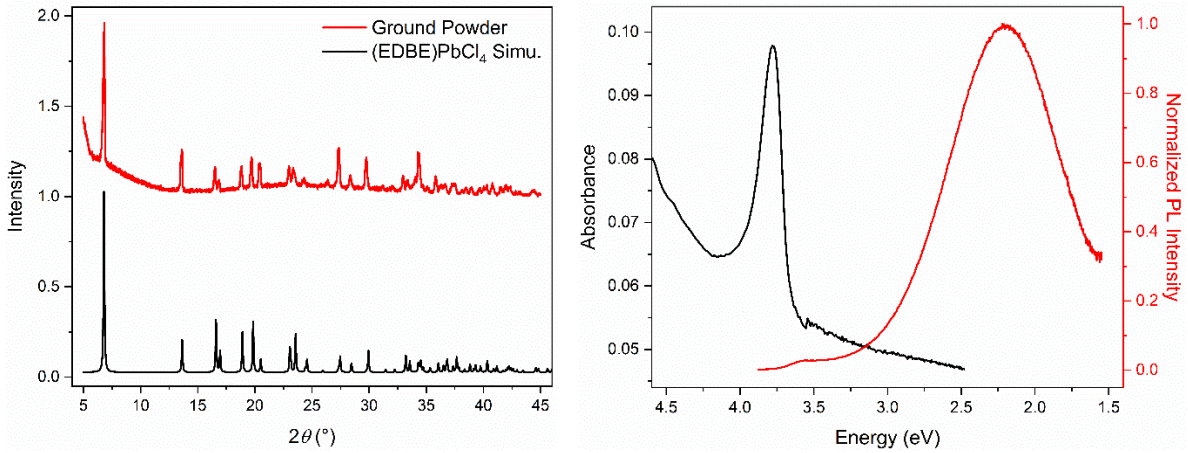

Figure S5. (Left) PXRD and (right) thin-film absorption (black) and powder PL (red) of $(EDBE)PbCl_4$

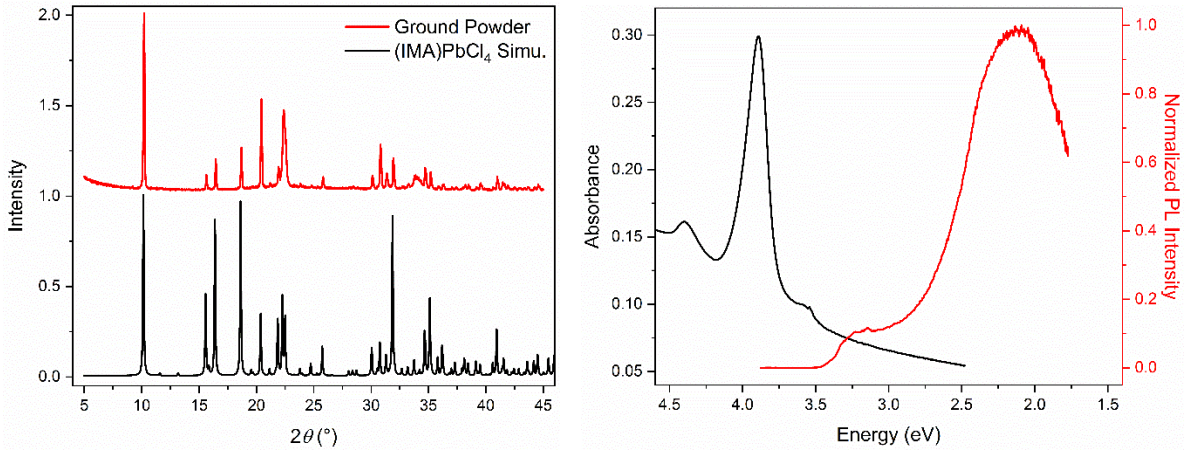

Figure S6. (Left) PXRD and (right) thin-film absorption (black), and powder PL (red) of $(IMA)PbCl_4$

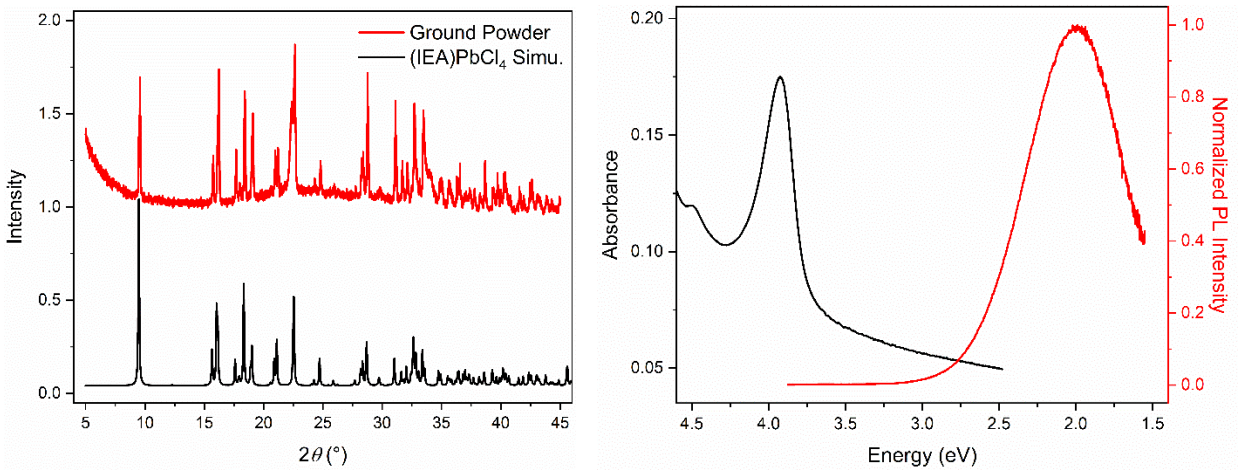

Figure S7. (Left) PXRD and (right) thin-film absorption (black) and powder PL (red) of $(IEA)PbCl_4$

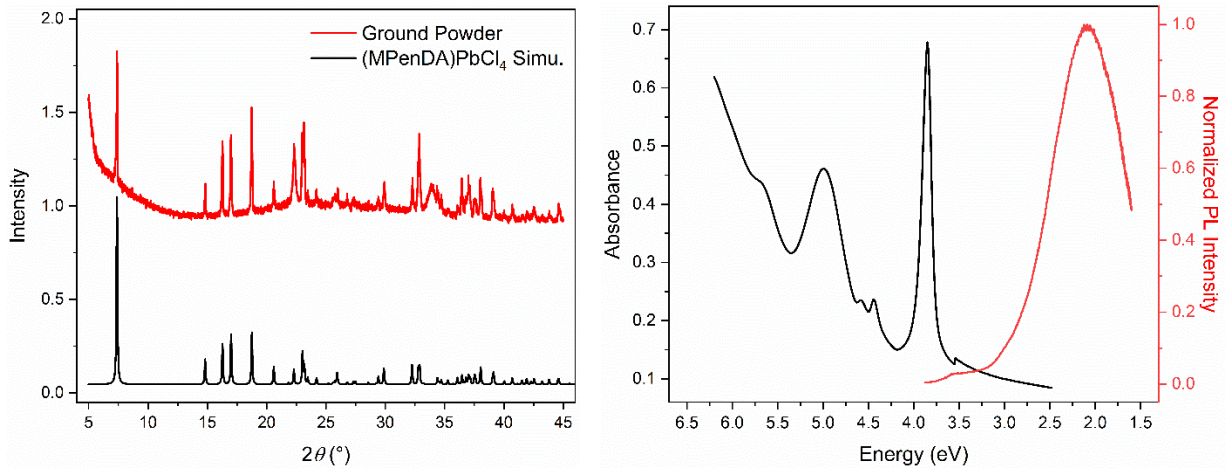

Figure S8. (Left) PXRD and (right) thin-film absorption (black) and powder PL (red) of $(MPenDA)PbCl_4$

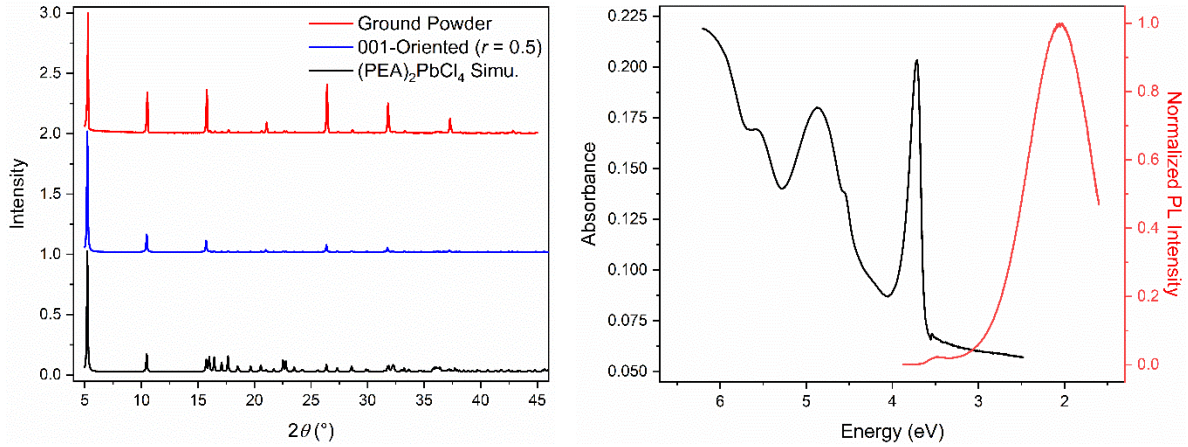

Figure S9. (Left) PXRD and (right) thin-film absorption (black), and powder PL (red) of $(PEA)_2PbCl_4$

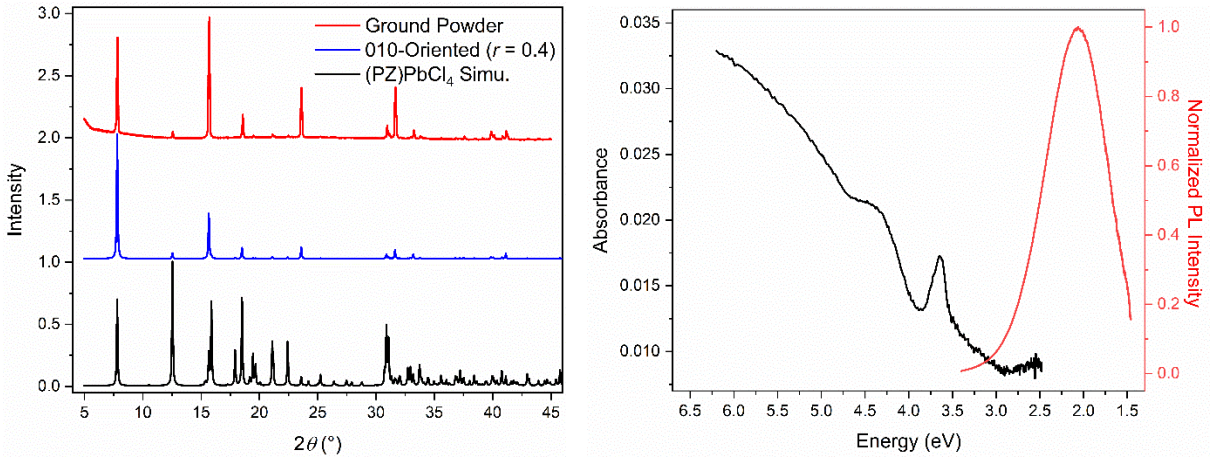

Figure S10. (Left) PXRD and (right) thin-film absorption (black) and powder PL (red) of $(PZ)PbCl_4$

Perovskite	*x*	*y*	CRI	CCT (K)
BIEA	0.42	0.45	82	3630
IMA	0.36	0.42	79	4895
IEA	0.42	0.46	80	3635
BDA	0.33	0.39	83	5600
MPenDA	0.35	0.41	83	4928
BzA	0.34	0.40	82	5319
PEA	0.37	0.43	82	4483
EDBE	0.32	0.39	80	6073
PZ	0.37	0.42	82	4602
API	0.42	0.43	87	3543

Table S4. CIE chromaticity coordinates for the Pb−Cl perovskites, which are identified by their organic cations. CRI: color rendering index; CCT: correlated color temperature

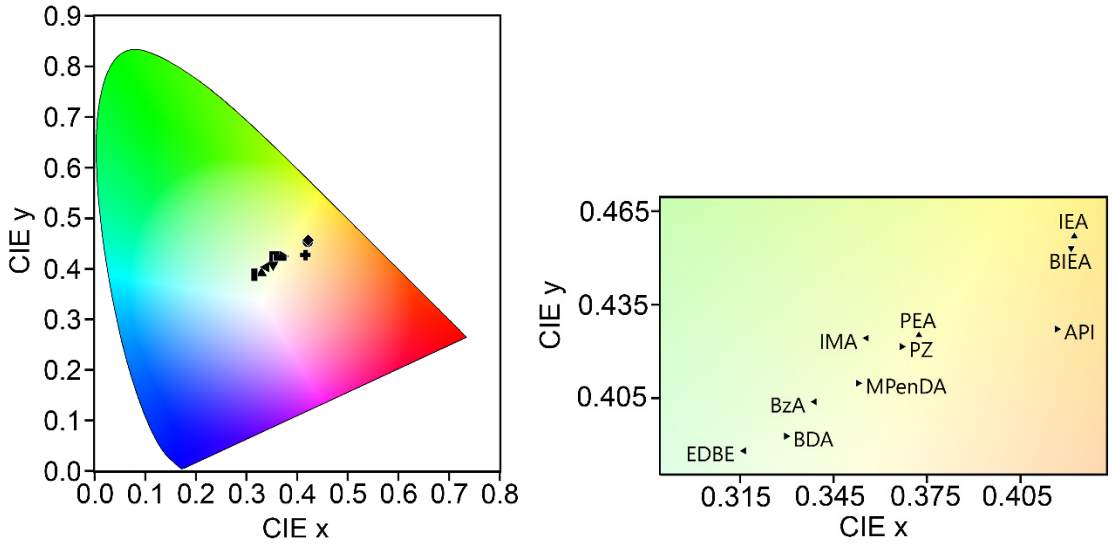

Figure S11. Full CIE chromaticity coordinate diagram (left) and a close-up (right) for the Pb−Cl perovskites

	Δ_{oct} ($\times 10^{-4}$)	σ^2_{oct}	λ_{oct}	S	Longest Pb–Cl Bond Length (Å)	Shortest Pb–Cl Bond Length (Å)	Longest Cl–Cl Distance (Å)	Shortest Cl–Cl Distance (Å)	Stokes Shift (eV)	Emission Maximum (eV)	fwhm (eV)
IMA	0.213	13.94	1.03	0.254	2.87	2.84	4.20	3.80	1.78	2.11	0.82
IEA	28.4	109.6	1.04	2.102	3.17	2.70	5.10	3.74	1.92	2.00	0.76
BDA	1.95	28.85	1.01	0.397	2.93	2.81	4.41	3.79	1.59	2.15	0.91
MPenDA	0.738	5.167	1.00	0.077	2.89	2.82	4.17	3.93	1.78	2.08	0.94
EDBE	0.558	800.8	0.91	7.177	2.88	2.83	5.40	2.89	1.58	2.20	0.91
PEA	8.31	18.17	1.02	0.194	3.03	2.75	4.24	3.92	1.66	2.05	0.87
BzA	0.411	22.10	1.01	0.257	2.89	2.84	4.28	3.84	1.67	2.13	0.90
BIEA	27.9	79.61	1.02	1.446	3.06	2.77	4.46	3.91	1.86	1.96	0.89
API	15.4	16.73	0.97	0.413	3.06	2.71	4.44	3.80	1.76	1.93	0.77
PZ	2.10	32.23	1.01	0.561	2.92	2.79	4.54	3.69	1.64	2.01	0.75

Table S5. Intraoctahedral distortion parameters and optical properties for the Pb–Cl perovskites, identified by their organic cations

	Pb–Pb Interoctahedral Distance (Å)	Cl–Cl Interoctahedral Distance (Å)	D_{out} (°)	Stokes Shift (eV)	Emission Maximum (eV)	fwhm (eV)
IMA	5.69	5.03	2.69	1.78	2.11	0.82
IEA	5.69	5.34	16.7	1.92	2.00	0.76
BDA	5.43	4.12	1.72	1.59	2.15	0.91
MPenDA	5.48	4.19	19.4	1.78	2.08	0.94
EDBE	5.40	5.40	16.9	1.58	2.20	0.91
PEA	5.58	4.25	6.42	1.66	2.05	0.87
BzA	5.37	3.95	0.00	1.67	2.13	0.90
BIEA	5.77	4.17	-	1.86	1.96	0.89
API	5.76	4.51	-	1.76	1.93	0.77
PZ	5.78	4.34	-	1.64	2.01	0.75

Table S6. Interoctahedral distortion parameters vs. optical properties for the Pb–Cl perovskites, identified by their organic cations

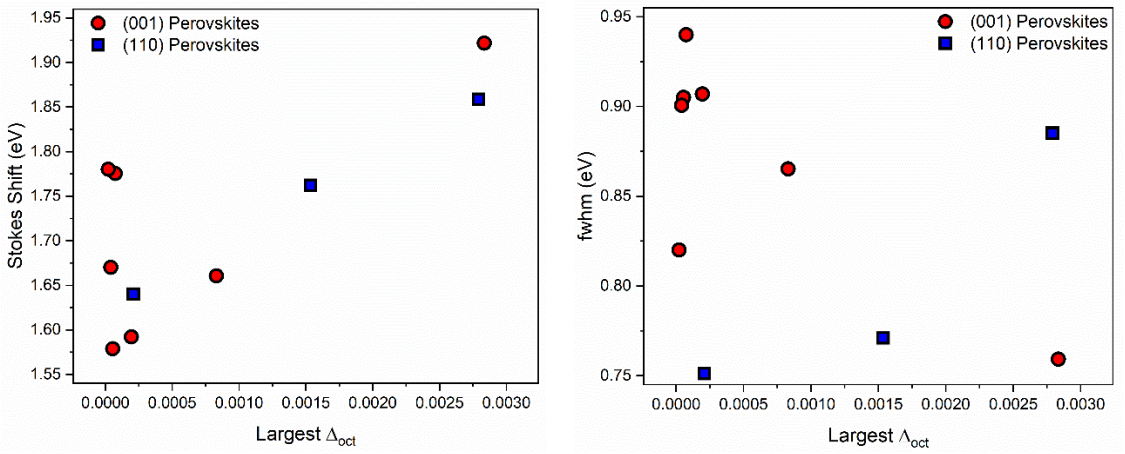

Figure S12. (Left) STE emission Stokes shift and (right) fwhm vs Δ_{oct} for the studied Pb–Cl perovskites

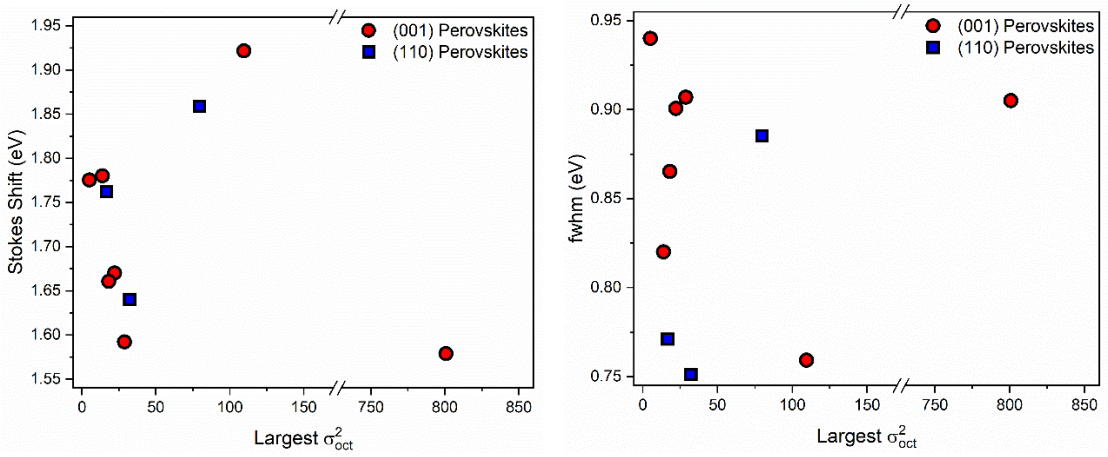

Figure S13. (Left) STE emission Stokes shift and (right) fwhm vs σ^2_{oct} for the studied Pb–Cl perovskites

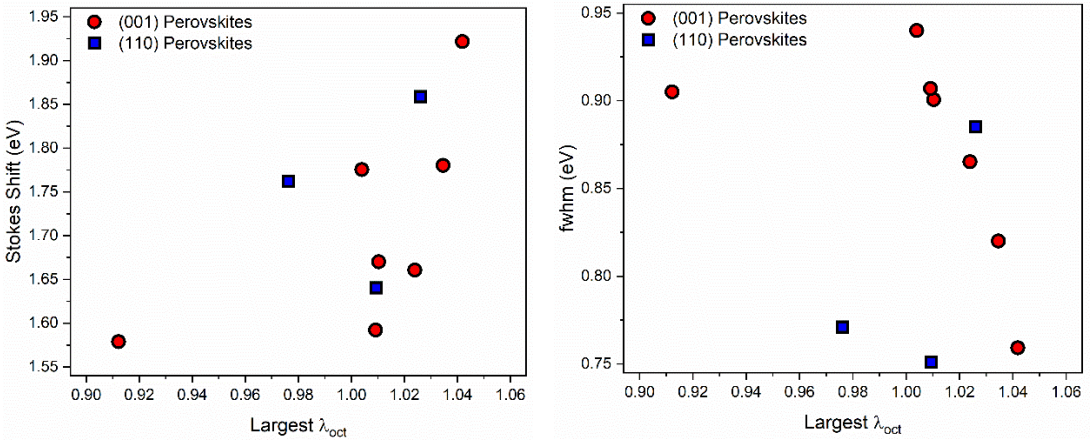

Figure S14. (Left) STE emission Stokes shift and (right) fwhm vs λ_{oct} for the studied Pb–Cl perovskites

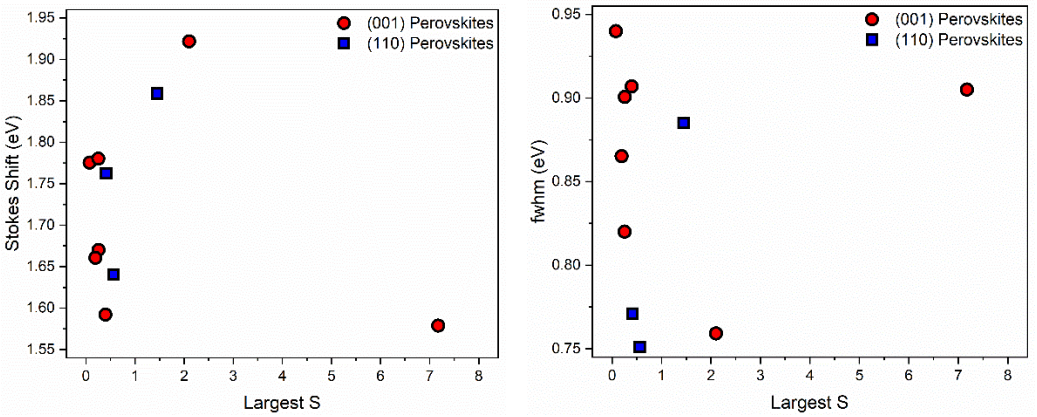

Figure S15. (Left) STE emission Stokes shift and (right) fwhm vs *S* distortion factor for the studied Pb–Cl perovskites

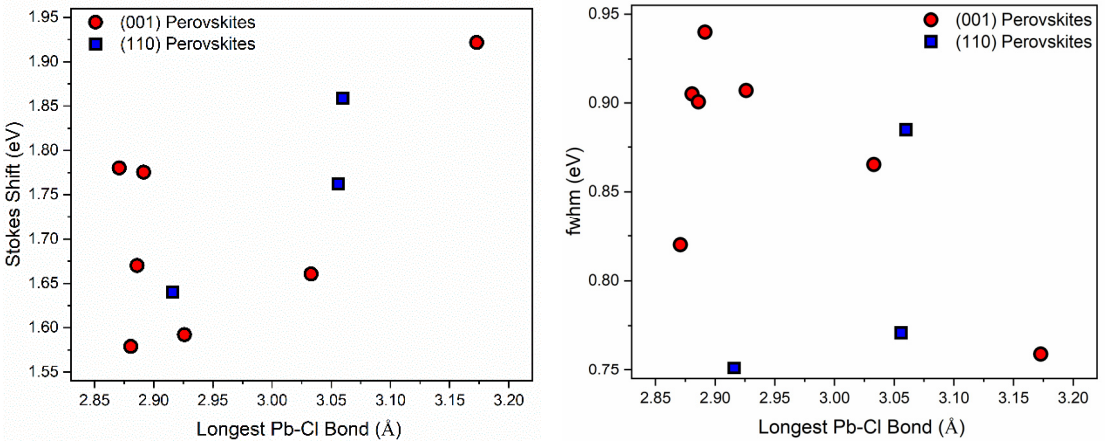

Figure S16. (Left) STE emission Stokes shift and (right) fwhm vs longest Pb–Cl bond for the studied Pb–Cl perovskites

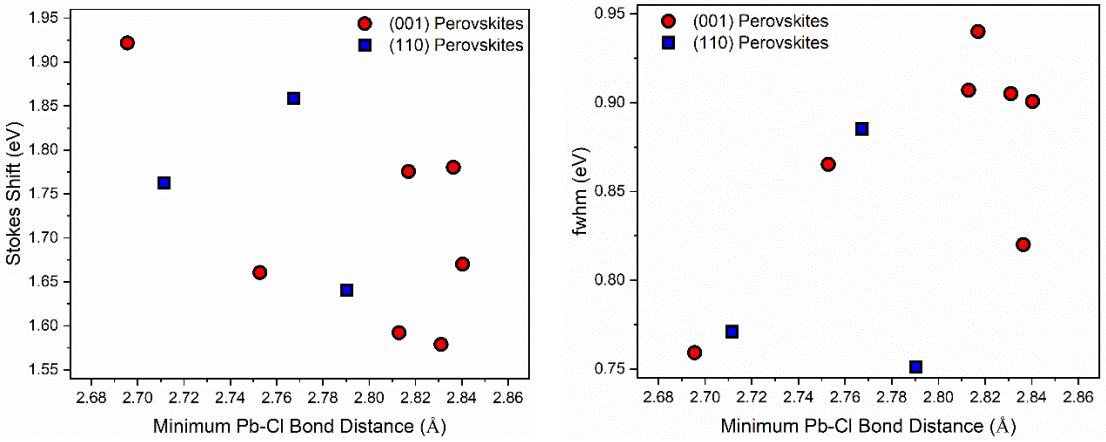

Figure S17. (Left) STE emission Stokes shift and (right) fwhm vs shortest Pb–Cl bond for the studied Pb–Cl perovskites

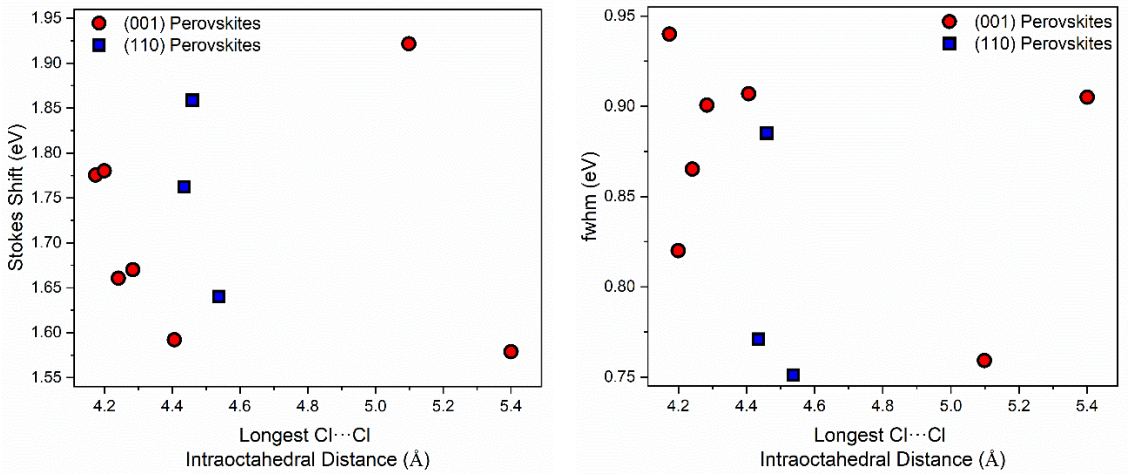

Figure S18. (Left) STE emission Stokes shift and (right) fwhm vs longest Cl–Cl intraoctahedral distance for the studied Pb–Cl perovskites

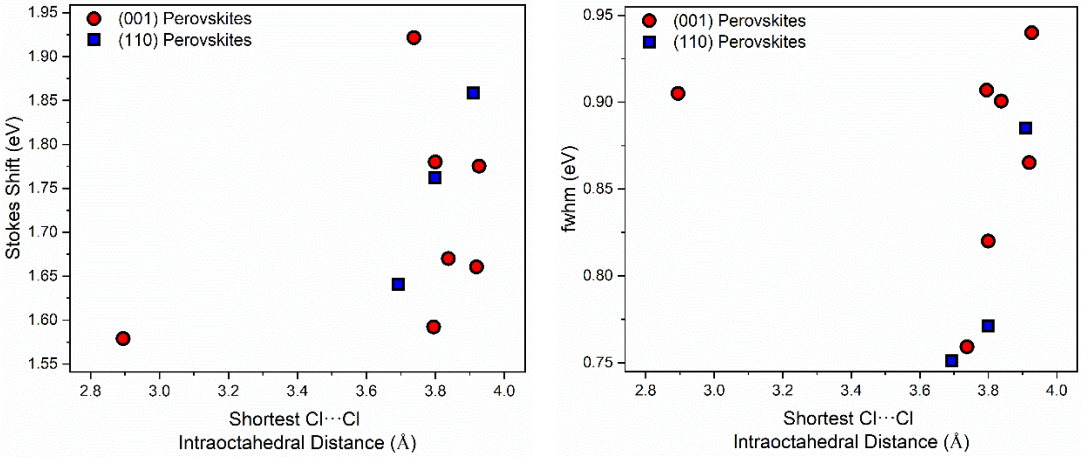

Figure S19. (Left) STE emission Stokes shift and (right) fwhm vs shortest Cl–Cl intraoctahedral distance for the studied Pb–Cl perovskites

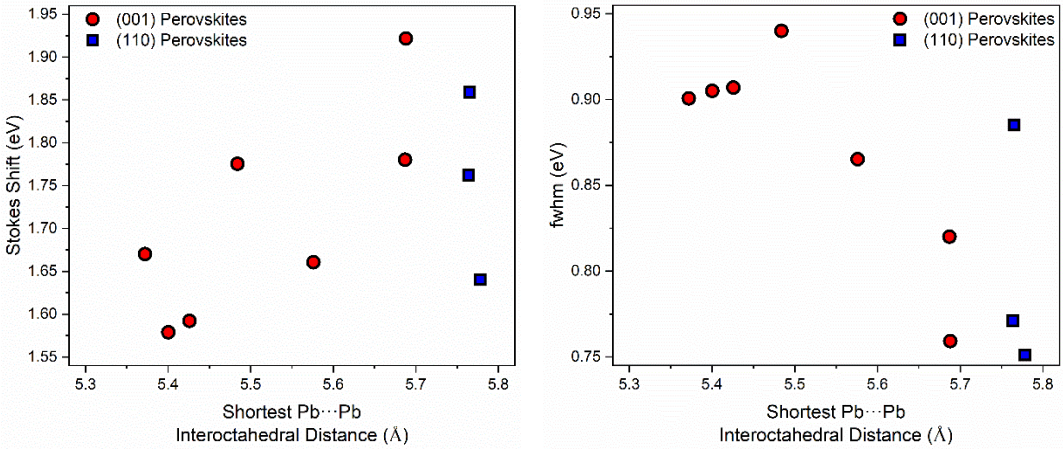

Figure S20. (Left) STE emission Stokes shift and (right) fwhm vs Pb–Pb interoctahedral distance for the studied Pb–Cl perovskites

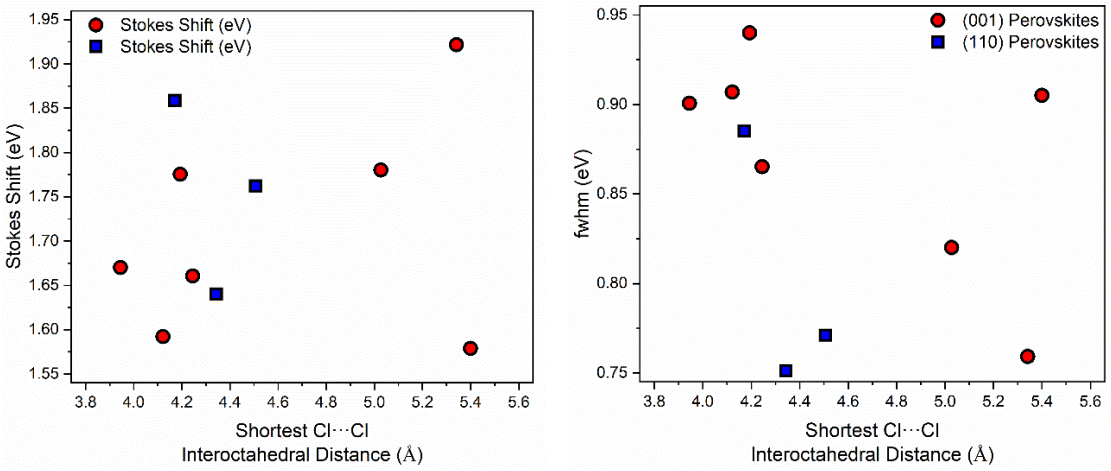

Figure S21. (Left) STE emission Stokes shift and (right) fwhm vs Cl–Cl interoctahedral distance for the studied Pb–Cl perovskites

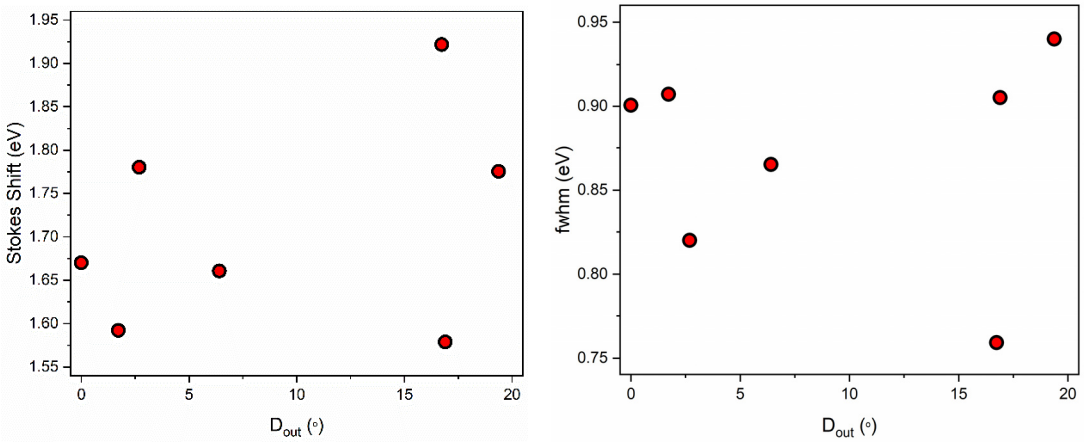

Figure S22. (Left) STE emission Stokes shift and (right) fwhm vs D_{out} for the studied (001) Pb–Cl perovskites

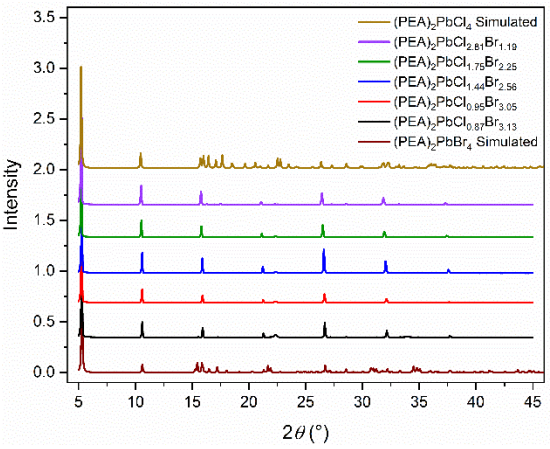

Figure S23. PXRD of $(PEA)_2PbCl_{4-x}Br_x$

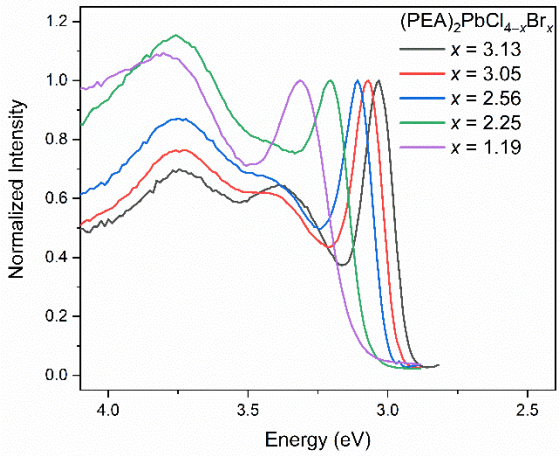

Figure S24. Photoluminescence excitation spectra of $(PEA)_2PbCl_{4-x}Br_x$

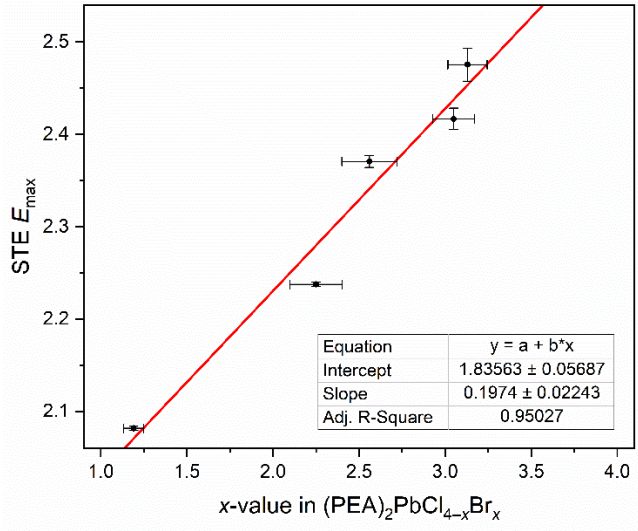

Figure S25. Linear correlation between x value in the formula $(PEA)_2PbCl_{4-x}Br_x$ vs STE emission maximum

Perovskite	x	y	CRI	CCT (K)	PLQE
$x = 0.00$	0.37	0.42	82	4463	(<1%)[21]
$x = 1.19$	0.34	0.39	86	5228	2%
$x = 2.25$	0.28	0.31	89	9414	3%
$x = 2.56$	0.23	0.23	NA	950000	4%
$x = 3.05$	0.21	0.17	NA	950000	3%
$x = 3.13$	0.19	0.12	NA	NA	5%
$x = 4.00$	0.19	0.10	NA	NA	3% (22%)[22-23]

Table S7. Chromaticity coordinates, CRI, CCT, and PLQEs of $(PEA)_2PbCl_{4-x}Br_x$. PLQE values from prior reports are noted in parentheses.

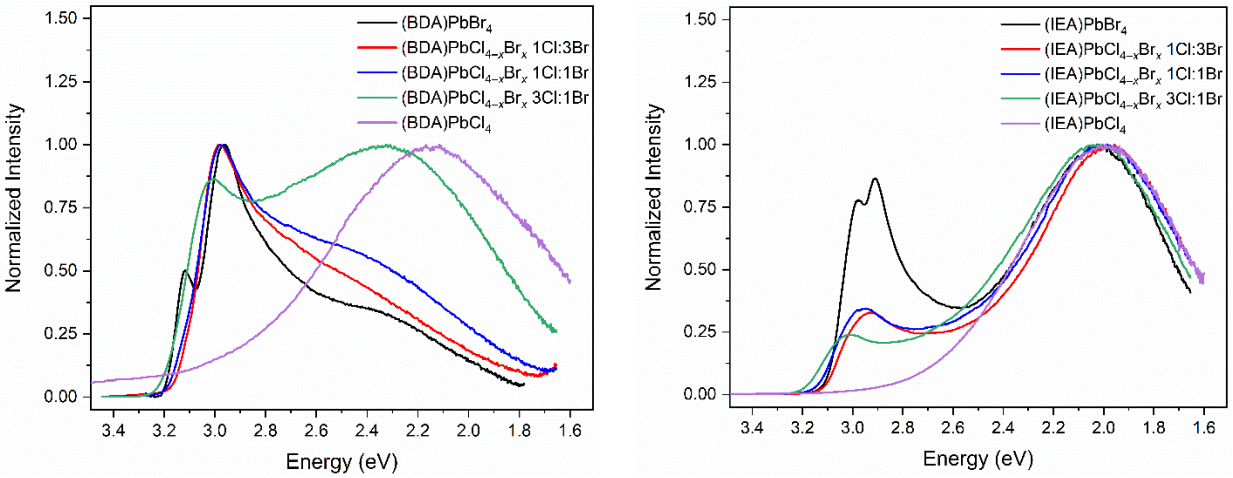

Figure S26. Evolution of PL spectra in (BDA)$PbCl_{4-x}Br_x$ (left) and (IEA)$PbCl_{4-x}Br_x$ (right) with halide ratio based on the halide ratio in the solution used to prepare the materials. The spectra are normalized to the most intense emission process.

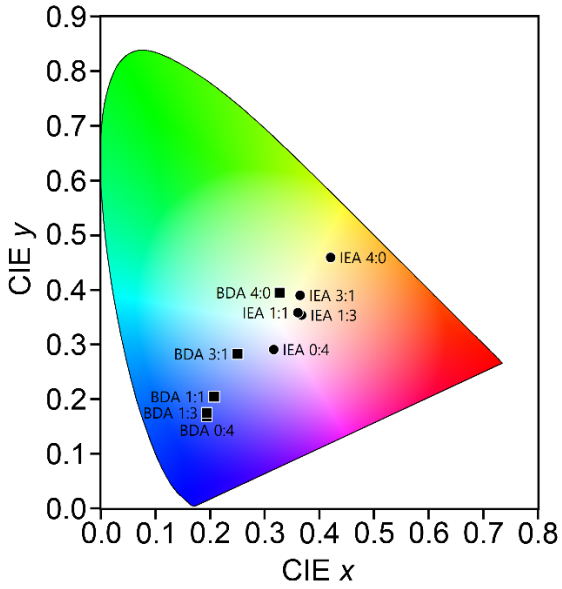

Figure S27. Chromaticity coordinate diagram for (BDA)$PbCl_{4-x}Br_x$ and (IEA)$PbCl_{4-x}Br_x$ with ratios indicating the Cl:Br ratio in the solutions used to prepare the materials.

Material	Solution Cl:Br Ratio	*x*	*y*	CRI	CCT (K)
(BDA)$PbCl_{4-x}Br_x$	0:4	0.20	0.17	NA	950000
	1:3	0.20	0.17	NA	950000
	1:1	0.21	0.20	NA	950000
	3:1	0.25	0.28	87	14771
	4:0	0.33	0.39	83	5600
(IEA)$PbCl_{4-x}Br_x$	0:4	0.32	0.29	87	6438
	1:3	0.37	0.35	91	4128
	1:1	0.36	0.36	91	4380
	3:1	0.37	0.39	87	4447
	4:0	0.42	0.46	80	3635

Table S8. Chromaticity coordinates, CRI, and CCT of (BDA)$PbCl_{4-x}Br_x$ and (IEA)$PbCl_{4-x}Br_x$

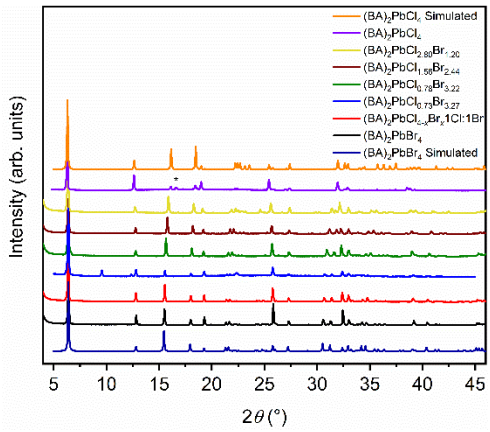

Figure S28. PXRD of $(BA)_2PbCl_{4-x}Br_x$. The peak marked with an asterisk is significantly more intense than in the simulated spectrum, which likely arises from preferential orientation of the sample.

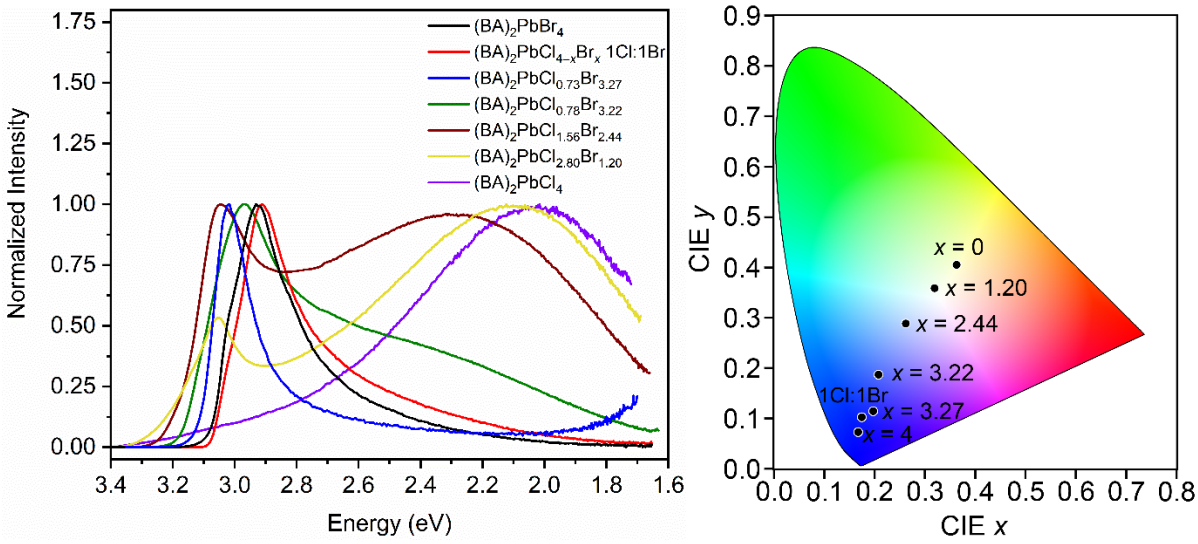

Figure S29. Evolution of PL (left) and CIE chromaticity coordinate diagram (right) for $(BA)_2PbCl_{4-x}Br_x$. "1:1 Cl:Br" denotes the ratio of concentrated hydrohalic acid volumes in the solution used to prepare the material.

Perovskite	*x*	*y*	CRI	CCT (K)	PLQE
x = 0.00	0.36	0.40	86	4645	(1%)[2]
x = 1.20	0.32	0.36	89	6063	1%
x = 2.44	0.26	0.29	90	12614	2%
x = 3.22	0.21	0.19	NA	950000	
x = 3.27	0.20	0.11	NA	NA	6%
1Cl:1Br	0.17	0.10	NA	NA	5%
x = 4.00	0.17	0.07	NA	NA	3% (0.4%)[22]

Table S9. Chromaticity coordinates, CRI, CCT, and PLQEs of $(BA)PbCl_{4-x}Br_x$. PLQE values from prior reports are noted in parentheses.

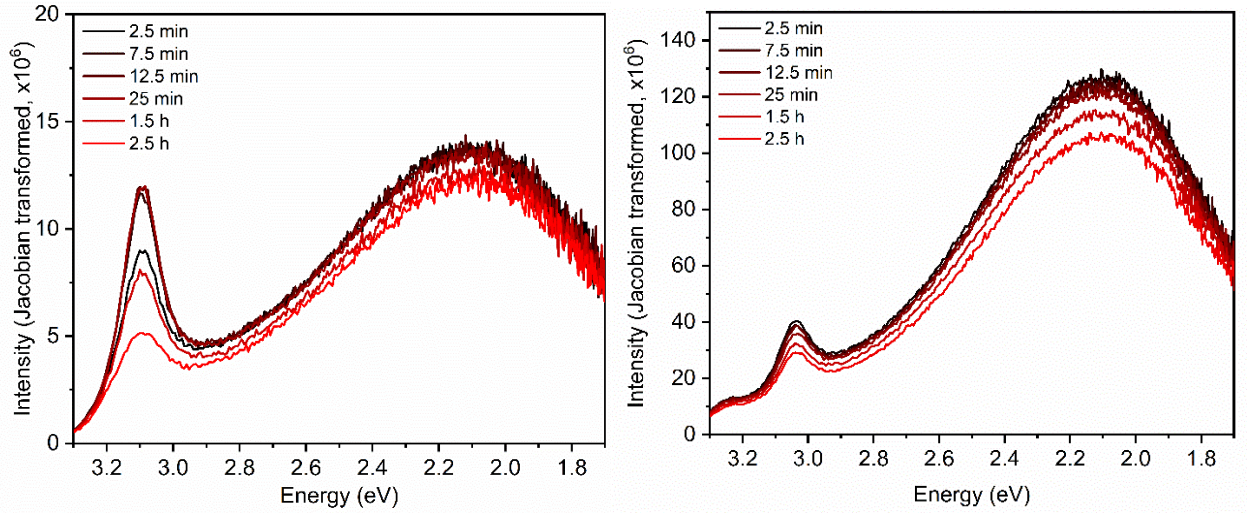

Figure S30. PL spectra of $(BA)_2PbCl_{2.80}Br_{1.20}$ (left) and $(PEA)_2PbCl_{2.81}Br_{1.19}$ (right) under continuous illumination by 340 nm light.

Illumination time	$(BA)_2PbCl_{2.80}Br_{1.20}$		$(PEA)_2PbCl_{2.81}Br_{1.19}$	
	x	*y*	*x*	*y*
2.5 minute	0.32	0.37	0.33	0.38
7.5 minute	0.32	0.35	0.33	0.38
12.5 minute	0.32	0.35	0.33	0.38
25 minute	0.32	0.35	0.33	0.38
1.5 h	0.32	0.36	0.34	0.39
2.5 h	0.32	0.36	0.34	0.39

Table S10. Chromaticity coordinates of $(BA)PbCl_{2.80}Br_{1.20}$ and $(PEA)_2PbCl_{2.81}Br_{1.19}$ under continuous UV illumination.

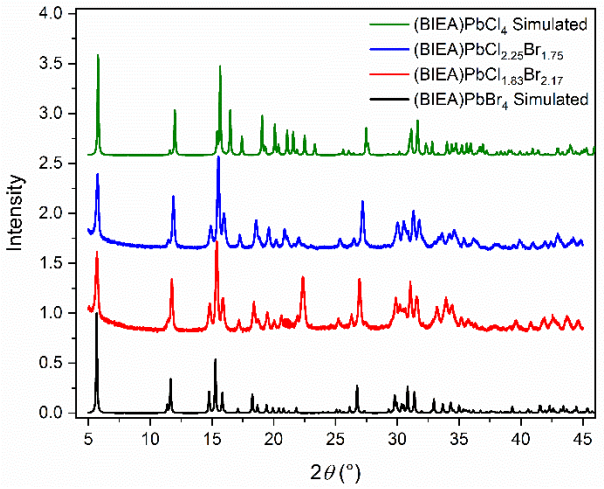

Figure S31. PXRD of $(BIEA)PbCl_{4-x}Br_x$

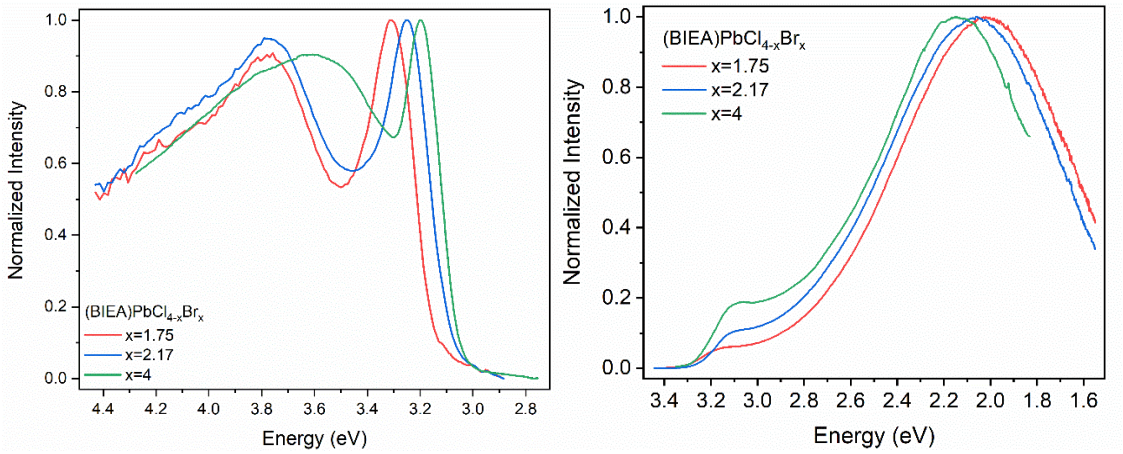

Figure S32. Photoluminescence excitation spectra (left) and emission spectra (right) of (BIEA)$PbCl_{4-x}Br_x$

Perovskite	*x*	*y*	CRI	CCT (K)
x = 0.00	0.46	0.42	93	2810
x = 1.75	0.38	0.42	84	4353
x = 2.17	0.36	0.41	84	4813
x = 4.00	0.34	0.39	81	5365

Table S11. Chromaticity coordinates, CRI, and CCT of (BIEA)$PbCl_{4-x}Br_x$

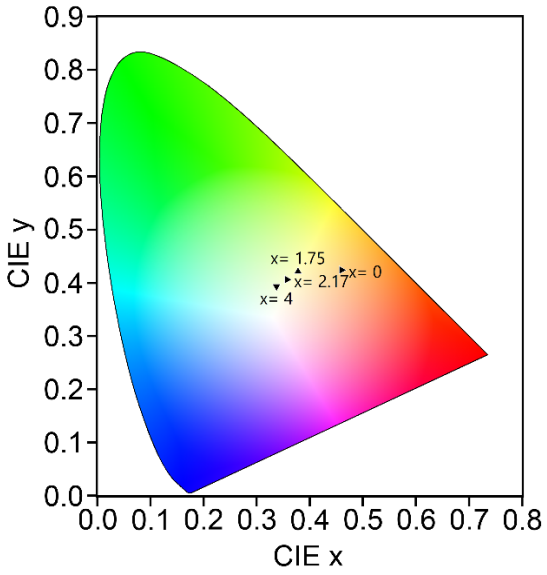

Figure S33. Chromaticity coordinate diagram of (BIEA)$PbCl_{4-x}Br_x$

References

(1) Dohner, E. R.; Jaffe, A.; Bradshaw, L. R.; Karunadasa, H. I., Intrinsic White-Light Emission from Layered Hybrid Perovskites. *J. Am. Chem. Soc.* **2014,** *136* (38), 13154-13157.
(2) Ji, C.; Wang, S.; Li, L.; Sun, Z.; Hong, M.; Luo, J., The First 2D Hybrid Perovskite Ferroelectric Showing Broadband White-Light Emission with High Color Rendering Index. *Adv. Funct. Mater.* **2019,** *29* (6), 1805038.
(3) Bruker-AXS (2018). *APEX3 and Saint*. Version 2018.1-0. Madison, W., USA.
(4) Krause, L.; Herbst-Irmer, R.; Sheldrick, G. M.; Stalke, D., Comparison of silver and molybdenum microfocus X-ray sources for single-crystal structure determination. *J. Appl. Crystallogr.* **2015,** *48* (1), 3-10.
(5) Sheldrick, G., Crystal structure refinement with SHELXL. *Acta Crystallogr., Sect. C* **2015,** *71* (1), 3-8.
(6) Sheldrick, G., A short history of SHELX. *Acta Crystallogr., Sect. A* **2008,** *64* (1), 112-122.
(7) Dolomanov, O. V.; Bourhis, L. J.; Gildea, R. J.; Howard, J. A. K.; Puschmann, H., OLEX2: a complete structure solution, refinement and analysis program. *J. Appl. Crystallogr.* **2009,** *42* (2), 339-341.
(8) Müller, P. H.-I., R.; Spek, A. L.; Schneider, T. R.; Sawaya, M. R., *Crystal Structure Refinement: A Crystallographer's Guide to SHELXL*. Oxford University Press: New York: 2006.
(9) Sheldrick, G., CELL_NOW, Version 2008/4; Georg-August-Universität Göttingen: Göttingen, Germany, 2008.
(10) Sheldrick, G. M. T. B., Madison, Wisconsin, USA.
(11) Petříček, V.; Dušek, M.; Palatinus, L., Crystallographic Computing System JANA2006: General features. In *Zeitschrift für Kristallographie - Crystalline Materials*, 2014; Vol. 229, p 345.
(12) Valenta, J., Photoluminescence of the integrating sphere walls, its influence on the absolute quantum yield measurements and correction methods. *AIP Advances* **2018,** *8* (10), 105123.
(13) Smith, M. D.; Jaffe, A.; Dohner, E. R.; Lindenberg, A. M.; Karunadasa, H. I., Structural origins of broadband emission from layered Pb-Br hybrid perovskites. *Chem. Sci.* **2017,** *8* (6), 4497-4504.
(14) Llunell, M. C., D.; Cirera, J.; Alemany, P.; Avnir, D.; Alvarez, S. *SHAPE: Program for the Stereochemical Analysis of Molecular Fragments by Means of Continuous Shape Measures and Associated Tools*, Universitat de Barcelona: 2010.
(15) Casanova, D.; Cirera, J.; Llunell, M.; Alemany, P.; Avnir, D.; Alvarez, S., Minimal Distortion Pathways in Polyhedral Rearrangements. *J. Am. Chem. Soc.* **2004,** *126* (6), 1755-1763.
(16) Cirera, J.; Ruiz, E.; Alvarez, S., Shape and Spin State in Four-Coordinate Transition-Metal Complexes: The Case of the d6 Configuration. *Chem. - Eur. J.* **2006,** *12* (11), 3162-3167.
(17) Pinsky, M.; Avnir, D., Continuous Symmetry Measures. 5. The Classical Polyhedra. *Inorg. Chem.* **1998,** *37* (21), 5575-5582.
(18) Lufaso, M. W.; Woodward, P. M., Jahn-Teller distortions, cation ordering and octahedral tilting in perovskites. *Acta Crystallogr., Sect. B* **2004,** *60* (1), 10-20.
(19) Robinson, K.; Gibbs, G. V.; Ribbe, P. H., Quadratic Elongation: A Quantitative Measure of Distortion in Coordination Polyhedra. *Science* **1971,** *172* (3983), 567-570.
(20) Sommerville, D., An Introduction to the Geometry of *n* Dimensions. Dover: New York, 1958; p 124.

(21) Thirumal, K.; Chong, W. K.; Xie, W.; Ganguly, R.; Muduli, S. K.; Sherburne, M.; Asta, M.; Mhaisalkar, S.; Sum, T. C.; Soo, H. S.; Mathews, N., Morphology-Independent Stable White-Light Emission from Self-Assembled Two-Dimensional Perovskites Driven by Strong Exciton–Phonon Coupling to the Organic Framework. *Chem. Mater.* **2017,** *29* (9), 3947-3953.
(22) Kawano, N.; Koshimizu, M.; Sun, Y.; Yahaba, N.; Fujimoto, Y.; Yanagida, T.; Asai, K., Effects of Organic Moieties on Luminescence Properties of Organic–Inorganic Layered Perovskite-Type Compounds. *J. Phys. Chem. C* **2014,** *118* (17), 9101-9106.
(23) Zhang, Y.; Liu, Y.; Xu, Z.; Ye, H.; Li, Q.; Hu, M.; Yang, Z.; Liu, S., Two-dimensional (PEA)2PbBr4 perovskite single crystals for a high performance UV-detector. *J. Mater. Chem. C* **2019,** *7* (6), 1584-1591.